INTRASEASONAL VARIABILITY OF THE INDONESIAN THROUGHFLOW

A Thesis

by

MARIANA CAROLINA NIEVA TAMASIUNAS

BS, University of Buenos Aires, Argentina, 2016

Submitted in Partial Fulfillment of the Requirements for the Degree of

MASTER OF SCIENCE

in

COASTAL AND MARINE SYSTEM SCIENCE

Texas A&M University-Corpus Christi
Corpus Christi, Texas

December 2019

December 2019

INTRASEASONAL VARIABILITY OF THE INDONESIAN THROUGHFLOW

A Thesis

by

MARIANA CAROLINA NIEVA TAMASIUNAS

This thesis meets the standards for scope and quality of
Texas A&M University-Corpus Christi and is hereby approved.

Toshiaki Shinoda, PhD
Chair

Chuntao Liu, PhD
Committee Member

Feiqin Xie, PhD
Committee Member

December 2019

ABSTRACT

Oceanic, atmospheric and land processes over the Maritime Continent (MC) play an important role in the Earth's climate system. In addition, a primary ocean current within the MC, the Indonesian Throughflow (ITF), is a major part of the global thermohaline circulation. This work investigates the intraseasonal variability (20-90 days) of the Indonesian Throughflow, which is primarily forced by the Madden-Julian Oscillation (MJO) using a 1/12° global HYbrid Coordinate Ocean Model (HYCOM) reanalysis and satellite altimeter data. To quantify the ITF transport variations over the MJO life cycle, composites of the ITF transport through the major straits in the Indonesian Seas are constructed. A prominent transport reduction during the MJO active phase is found in all major straits. Also, a transport enhancement during the suppressed phase, that is comparable to the reduction, is evident. As a result, the net effect of the MJO on the ITF transport is very small because of the cancellation of the enhancement and reduction. Upper ocean variability associated with the MJO in the Indonesian Seas is then compared with major atmospheric variables. During both active and suppressed phases of the MJO, surface winds over the MC are consistent with the spatial pattern of MJO-induced upper ocean currents. The role of remote ocean response in the ITF variations is further investigated. During the active phase, sea surface height and along-shore current anomalies generated in the central Indian Ocean by the MJO forcing propagate along the coast of Java and Sumatra as a coastal Kelvin wave, which largely influences the ITF transport at exit passages and Makassar strait. During the suppressed phase, the propagation of Kelvin wave is not clearly detected in the composite, suggesting that local winds over the MC are mostly responsible for the ITF variation. The effect of Kelvin waves on the ITF variability is further examined for MJO events observed during DYNAMO field campaign. The propagation of Kelvin waves from the equatorial Indian Ocean to the ITF exit

passages is evident during both active and suppressed phases, suggesting that upwelling Kelvin waves contribute to the ITF transport through the exit passages for some MJO events.

DEDICATION

To my beloved mother Susana, who has supported me since day one. Her love, guidance and advice have led me across the globe, but my heart will always be next to her.

To my boyfriend and life partner Justin, who has been my rock and my strength along the way, and who believes in me unconditionally.

To my extended family, friends and colleagues, for making the road fun and enjoyable.

ACKNOWLEDGEMENTS

I would like to thank my committee chair, Dr. Shinoda, and my committee members, Dr. Liu and Dr. Xie, for their guidance and support throughout this research.

This research is supported by NOAA grants NA17OAR4310256 and NA15OAR431074, NSF grant OCE-1658218, and NASA grant NNX17AH25G.

TABLE OF CONTENT

LIST OF FIGURES

FIGURES PAGE

LIST OF TABLES

TABLES PAGE

1. INTRODUCTION

Oceanic and atmospheric processes over the Maritime Continent (MC, Fig. 1) play a key role on Earth's climate and global ocean circulation. As the MC is located on the warmest (~28°C) ocean area in the world, called the "Tropical Warm Pool" or the "boiler box" of the Tropics (Ramage, 1968), the area has a potential to transfer a large amount of energy to the atmosphere, and thus ocean variability in this region affects climate variations across the globe on multiple time scales (Neale and Slingo, 2003). Such climate variability includes changes in the Walker Circulation through frequent convective storms (Keenan et al., 2000), the El Niño Southern Oscillation (ENSO) (Lau and Chan, 1983), the Indian Ocean Dipole (Saji et al., 1999), and the Madden-Julian Oscillation (MJO; Madden and Julian, 1971, 1972). Therefore, it is important to investigate the upper ocean processes over the MC region that could largely affect the sea surface temperature (SST).

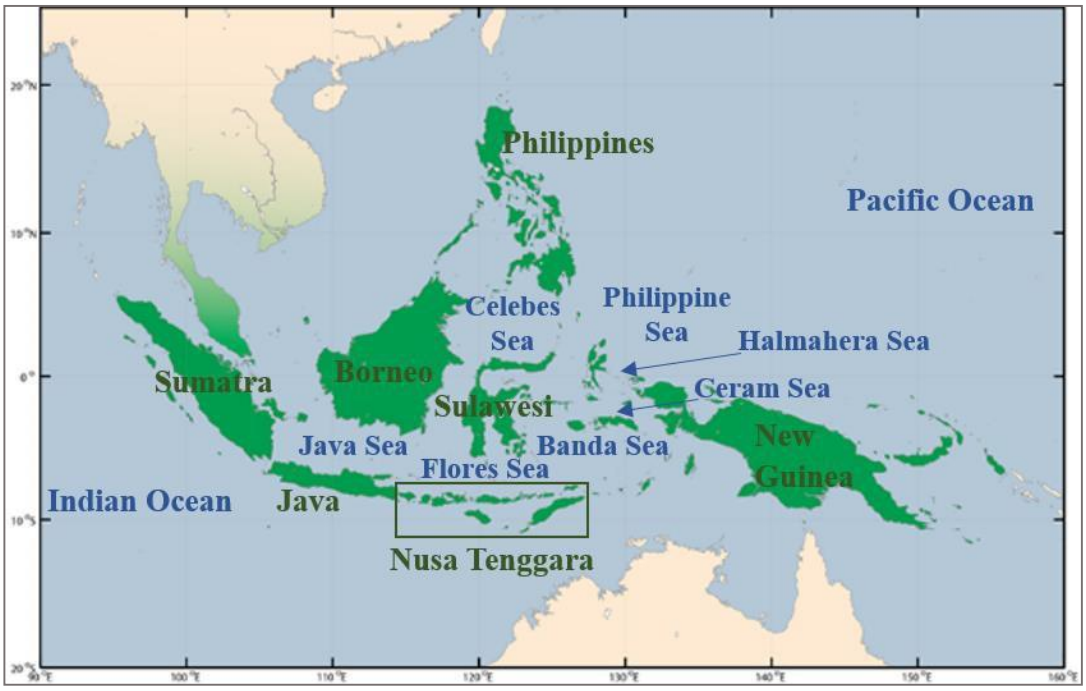

Fig. 1. The Maritime Continent (green area). Adapted from: http://www.bom.gov.au/climate/about/tropics/maritime-continent.shtml)

The MC includes many small islands and narrow straits (Fig. 1). There, atmospheric convection is very intense, and it provides a critical heat source for the atmospheric circulation on the planetary scale. Larger-scale organization of thunderstorm activity as well as strong sea-breeze is strongly influenced by the orography (Neale and Slingo, 2003). In addition, the convection over the MC could be described as a part of the planetary monsoon system (Lau and Chan 1983b, Meehl 1987, and McBride 1998). On the interannual timescale, ENSO can modulate the rainfall over the MC (Philander, 1985). During the ENSO warm phase, strong convection shifts to the central Pacific, leading to the rainfall suppression over the MC (e.g., Qian, 2008).

Ocean circulation over the MC region is a portion of the upper branch of the global ocean thermohaline circulation. The Indonesian Throughflow (ITF, Fig. 2), which is a major current within the MC area, carries about 15 Sv of waters from Pacific to Indian Ocean (Sprintall et al., 2009) and it flows through the complex bathymetries in the MC. This is a well-known area for the transformation and formation of very distinct water masses due mainly to strong tidal mixing (Koch-Larrouy et al., 2008). Waters in the Indonesian Seas are fresher than those of the Indian Ocean (Gordon et al., 1997) and they contribute significantly to the upwelling of cold water in the global conveyor belt. The waters carried by ITF further affect larger areas of the Indian Ocean. They flow across the tropical Indian Ocean and a significant portion of ITF waters enter the Agulhas Current system, where they are identified in many Agulhas eddies in the Atlantic (Song et al., 2004). Also, some of the waters in the Indonesian seas flow southward, providing a water source for the Leeuwin Current along the western coast of Australia (Gentilli, 1972).

The ITF varies on several different time scales. For example, Meyers (1996) found that the ITF is stronger during La Niña and weaker during El Niño, with the magnitude of the variation of

about 5 Sv. It is suggested that during the ENSO, a westerly wind anomaly in the equatorial Pacific Ocean causes the decrease of the sea level in the western Pacific, which results in the decrease of the pressure gradient between the western Pacific and the eastern Indian Ocean, and thus the ITF weakens. This result is further supported by Wijffels and Meyers (2004) and Rejeki et al. (2017). On the other hand, other studies suggest that the interannual variability of the ITF is mainly governed by the Indian Ocean dynamics (Masumoto, 2002) including that associated with the Indian Ocean Dipole (Sprintall and Revelard, 2014; Liu et al., 2015) that counter the ENSO effect when the two occur simultaneously. On a decadal scale, it is suggested that the weakening of the Walker Circulation due to a warming climate (Vecchi et al., 2006; Tokinaga et al., 2012) weakens the ITF (Wainwright et al., 2008; Sen Gupta et al., 2012).

The seasonal variation in the ITF transport is partly driven by the Asian-Australian Monsoon winds (Meyers, 1995). For example, the ITF is maximum during the Australian southeast monsoon, during which southearly winds blow over the MC causinga strong Ekman divergence in the Indonesian Seas (Sprintall et al. 2009, Gordon and Susanto, 2001). Shinoda et al., (2012) demonstrated that the southward ITF transport is reduced during April–May and October–November, which is caused by the propagation of coastal Kelvin waves generated by the Wyrtki jet in the tropical Indian Ocean while the recovery of the transport during January–March originates from upper-ocean variability linked to annual Rossby waves in the Pacific Ocean.

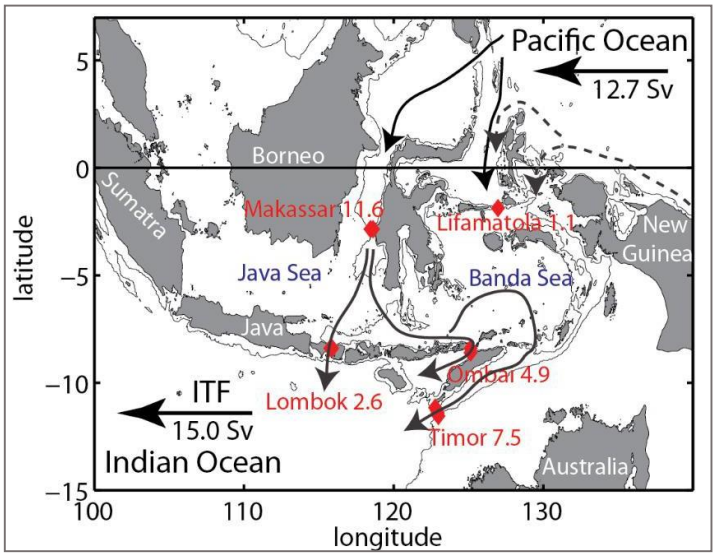

Fig. 2. The Indonesian Throughflow and its associated transports on the MC major straits. Adapted from Sprintall et al., 2009.

Prominent intraseasonal variability of the ITF is also identified in recent studies. Qiu et al., (1999) found that the intraseasonal signals along the Sumatra/Java coasts were induced remotely by coastal Kelvin waves with the period of 50-85 days that are generated by intraseasonal anomalous surface zonal winds in the central equatorial Indian Ocean. Schiller et al., (2010) further demonstrated that the signals of intraseasonal Kelvin wave are detected as far east as the Banda Sea and that the intraseasonal variability in the region is also forced by local winds. They also state that part of the intraseasonal wave energy is transmitted through Lombok Strait northward to Makassar Strait, causing a decrease in the ITF transport. Pujiana et al. (2013) provided the detailed description of Kelvin wave characteristics between the Lombok and Makassar Straits. It is suggested that equatorial westerly wind bursts in the Indian Ocean associated with the MJO generate these intraseasonal coastal Kelvin waves that penetrate into the Indonesian seas. A recent study by Napitu et al., (2019) further examined the ITF transport variation through the Makassar Strait associated with the MJO based on the analysis of mooring data. They reported that the

Makassar Strait throughflow transport is increased during the MJO suppressed phase, while the transport is decreased during the active phase.

While these previous studies on ITF intraseasonal variability suggest some important oceanic processes that could influence the ITF, the ITF transport variations through most major straits in the Indonesian Seas over the life cycle of the MJO have not been quantified. Most of these studies focus on the ITF transport through the Makassar Strait, and the variation of ITF transport on the intraseasonal time scale through other major straits is not well understood. In addition, these studies mostly investigate the impact of MJO during the active phase, and the MJO influence on ITF transport during the suppressed phase is not emphasized, and thus the net effect of MJO on the overall ITF transport is not well known.

A major goal of this study is to quantify the intraseasonal variability of overall ITF transport through major straits over the MC. As described above, a large portion of ITF intraseasonal variability is caused by the MJO. The MJO is the dominant mode of the intra-seasonal variability in the tropics, and it has an important impact on the global weather and climate (e.g. Zhang, 2005). It is a basin-scale perturbation characterized by deep convective clouds and low-level winds with 20 to 90-day period that propagates eastward over the Indo-Pacific Oceans (Fig. 3). As it has been mentioned before, larger-scale intraseasonal activity can be largely modified over the MC. When the MJO propagates over the region in its mature phase, it is modulated by the underlying surface properties and then moves to the West Pacific. For example, the MJO tends to propagate over the MC during the MJO suppressed phase when the SST in the Indonesian Seas is warmer (Napitu et al., 2017). Since the variations of ITF could largely modify the SST in the MC region, it is crucial to investigate ITF variability which could further feedback on the MJO propagation.

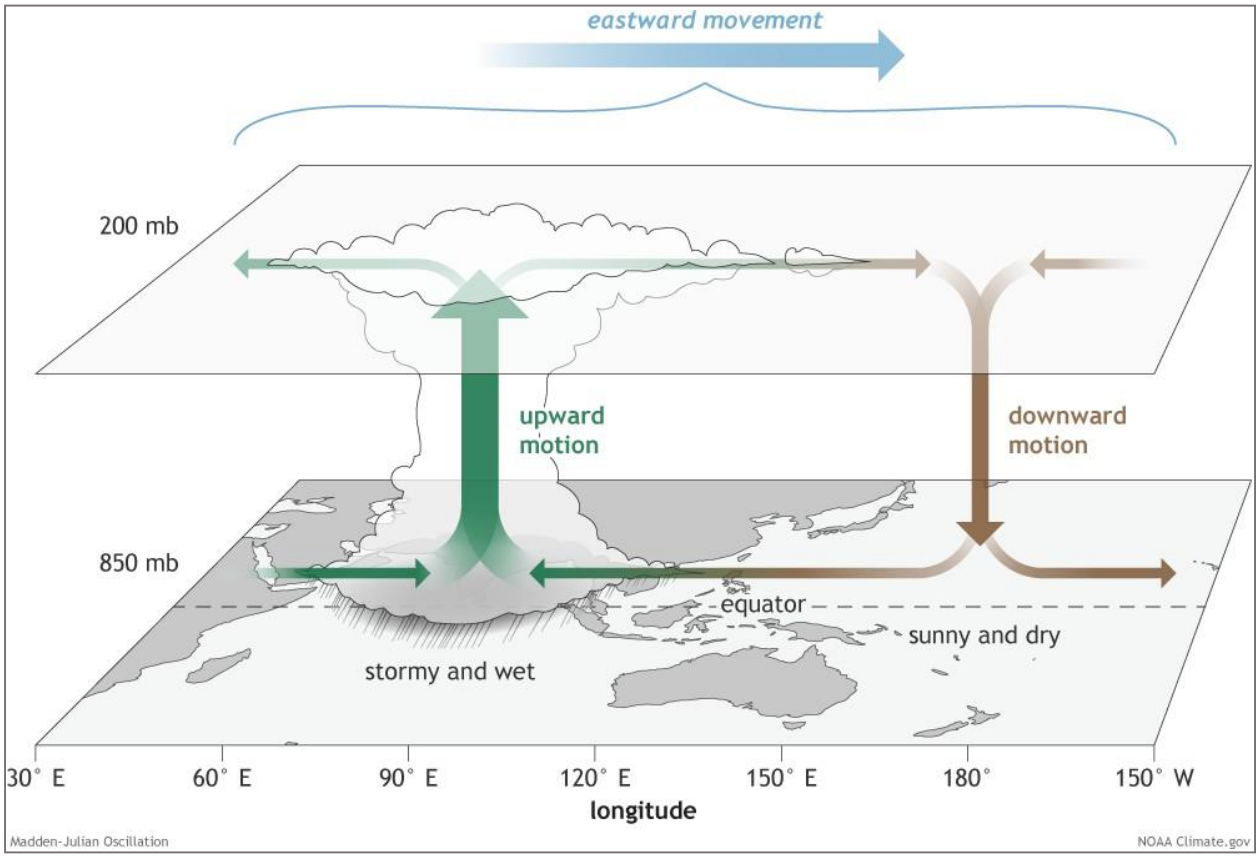

Fig. 3. The surface and upper-atmosphere structure of the MJO for a period when the enhanced convection is centered in the Indian Ocean and the suppressed convection is centered over the west-central Pacific Ocean. Horizontal arrows indicate wind anomalies. The entire system moves eastward over the warm pool. (https://www.climate.gov/news-features/blogs/enso/what-mjo-and-why-do-we-care)

Until recently, it has been difficult to describe ITF transports through all major straits in the Indonesian Seas due to the lack of in-situ observations as well as other reliable high-resolution data. A new high-resolution (1/12°) global ocean reanalysis has been recently created, which can provide a useful tool to investigate the upper ocean variability including the ITF. In this study, we analyze the high-resolution ocean reanalysis along with the satellite and in-situ data to examine the effect of the MJO on the upper ocean currents and the ITF transport.

The following specific questions will be addressed in this study:

I) How does the transport of the ITF through major straits in the Indonesian Seas vary during the MJO active and suppressed phases, and what is the net effect of the MJO on the overall ITF transport?

II) How does the remotely-forced ocean variability associated with the MJO contribute to the ITF transport in major straits?

2. DATA AND METHOD

2.1 Data

2.1.a. High resolution ocean reanalysis data

This study used the ocean reanalysis consisting of the 0.08° Hybrid Coordinate Ocean Model (HYCOM; Bleck, 2002) and the Navy Coupled Ocean Data Assimilation (NCODA; Cummings 2005, Cummings and Smedstat, 2013). This reanalysis product is referred to as "HYCOM reanalysis" hereafter. The NCODA includes remotely sensed sea surface height (SSH), SST and sea ice concentration along with in-situ surface and subsurface observations of temperature and salinity. The details of the NCODA data are described in Cummings (2005) and the explanation of the assimilation method is found in Cummings and Smedstad (2013). HYCOM combines the z-level coordinate for the unstratified sea, the isopycnal coordinate in the open ocean and a terrain-following one for coastal areas. The details about HYCOM can be found in Bleck (2002). The daily mean values of velocity and sea surface height for the period 2004–2015 are used in this study, which includes many MJO events. Also, the period covers one of the major in-situ observations of ITF: International Nusantara STratification ANd Transport program (INSTANT) during 2004-2006. The HYCOM reanalysis will be validated against in-situ and

satellite observations over the MC region and the Central Indian Ocean in this study, while it has been extensively validated in other areas (Yu et al., 2015, Thoppil et al., 2016).

2.1.b. In-situ and satellite data

This study employs both satellite and in-situ data. The in-situ data includes those collected during the INSTANT program. This program (Sprintall et al., 2004) was designed to directly measure the ITF in major straits in the Indonesian Seas. It consisted of a 3-year deployment of an array of moorings and coastal pressure gauges to measure sea level and full-depth in situ velocity, temperature, and salinity since August 2003. The moorings were located on the ITF main pathway passages: Makassar, Lombok and Ombai Straits and Timor and Lifamatola Passages (Fig. 4). This study employed hourly velocity time series from the two Makassar Strait ADCP moorings for the comparison with HYCOM reanalysis.

The data collected during the Cooperative Indian Ocean Experiment on Intraseasonal Variability (CINDY)/ Dynamics of the Madden-Julian Oscillation (DYNAMO) field campaign (Yoneyama et al., 2013, Zhang et al., 2013) are also used. The upper ocean data were obtained from multiple instruments including CTD profiles, ADCP moorings, XBT launchings, sea gliders. Three MJO events were observed during the campaign in boreal fall/winter 2011/12. Strong upper ocean response to those MJO events was measured during the campaign (e.g., Moum et al. 2014, Shinoda et al. 2013, 2017). The upper ocean velocity data measured by ADCPs are used in this study. The velocity data from the Research Moored Array for African–Asian–Australian Monsoon Analysis and Prediction (RAMA) program (McPhaden et al., 2009) was also employed.

Sea surface height (SSH) data from Archiving, Validation, and Interpretation of Satellite Oceanographic (AVISO) are used (National Center for Atmospheric Research Staff (Eds), 2016).

AVISO SSH data have been created based on the satellite altimetry measurements from TOPEX/Poseidon, Envisat, Jason-1, and OSTM/Jason-2, which provides daily SSH values on 0.25° grids. NOAA Interpolated Outgoing Longwave Radiation (OLR) data (Liebmann and Smith, 2006) are used, which are presented on a 2.5° x 2.5° global grid. Daily winds at 10 m height obtained from the National Centers for Environmental Prediction (NCEP) Climate Forecast System Reanalysis (CFSR) (Saha et al., 2010) for the period of 2004-2010 and the Climate Forecast System Version 2 (CFSv2) (Saha et al., 2014) for the period of 2011-2015 are also used.

2.2 Composite analysis

To detect common processes acting in most MJO events, oceanic and atmospheric variables derived from the HYCOM reanalysis and observations for the period 2004-2015 are used to form the composite of the MJO, following the method used in Guan et al., (2014). The composite is based on the Real-time Multivariate MJO (RMM) Index (Wheeler and Hendon, 2004), a season-independent index that can be used to detect the MJO events. This index is based on a pair of empirical orthogonal functions (EOFs) for OLR and wind anomalies, and it describes an MJO event as an eight-phase cycle. The principal component time series that are a result of the projection of observed data onto the multiple-variable EOFs, vary mostly on the intraseasonal time scale of the MJO only. For the purpose of this study, an MJO event was defined as the period of time during which the RMM MJO index magnitude is greater than 1 for at least thirty consecutive days. The climatology of all variables was calculated as the result of the harmonic analysis of the daily mean values for the 2004-2015 period. And after that, the composite is constructed by averaging the anomalies in respect of the climatology of the variable for each MJO phase.

3. RESULTS

3.1 Comparison of HYCOM reanalysis with observations

To validate the HYCOM reanalysis over the MC region, velocities in the major straits or passages of the ITF in the HYCOM reanalysis are first compared with those from the INSTANT observations for the period 2004-2006. Mean transport values as well as the vertical structures of mean currents are calculated for all major straits. The mean transport values for all major straits (Fig. 4) agree well with values estimated from observations (Table 1).

	Transports (Sv)	
	HYCOM reanalysis	**Observations**
Makassar	-11.05	-11.6 (Gordon et al., 2008), -12.7 (Susanto et al, 2012)
Lombok	-2.79	-2.6 (Sprintall et al., 2009)
Ombai	-4.17	-4.9 (Sprintall et al., 2009)
Timor	-5.80	-7.5 (Sprintall et al., 2009)
Lifamatola	$+9x10^{-3}$	-1 (van Aken et at., 2009)

Table 1. Transport values obtained from HYCOM reanalysis data (left) and based on observations (right) in the major straits in the Indonesian Seas for the period 2004-2006. Negative values indicate a transport from Pacific to Indian Oceans.

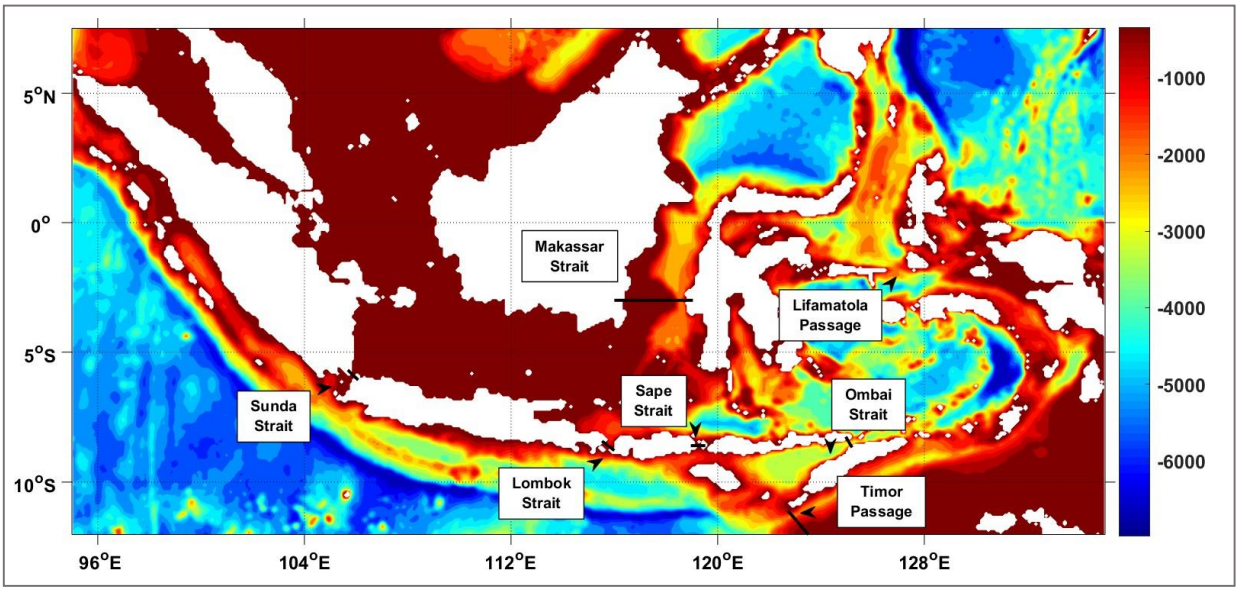

Fig. 4. The 1/12° global HYCOM topography (m) for the Indonesian Seas and the major straits.

The vertical structures of mean currents across the major straits also agree well with observations (Fig. 5). For example, the location of the maximum mean current from the HYCOM reanalysis is quite similar to that for the observations for Lombok Strait (Fig. 5a), although the current is a little weaker (~0.2 cm/s). Mean along-strait currents for Ombai Strait (Fig. 5b) are also similar to the observations, including those in the deeper area. For Timor Passage (Fig. 5c) the agreement is very good for the entire column. Both the magnitude and the vertical structure of the mean velocity are very similar to those found in observations.

The time series of along-strait velocity at the Makassar strait was compared with INSTANT observations (Fig. 6). The reanalysis is able to capture the variability of the Makassar Strait Throughflow reasonably well, including its semi-annual and intraseasonal variations. For example, the decrease of southward along-strait velocity observed during April-June 2005 is well reproduced by the HYCOM analysis. This intraseasonal fluctuation of along-strait velocity is associated with the MJO event observed during this period (not shown).

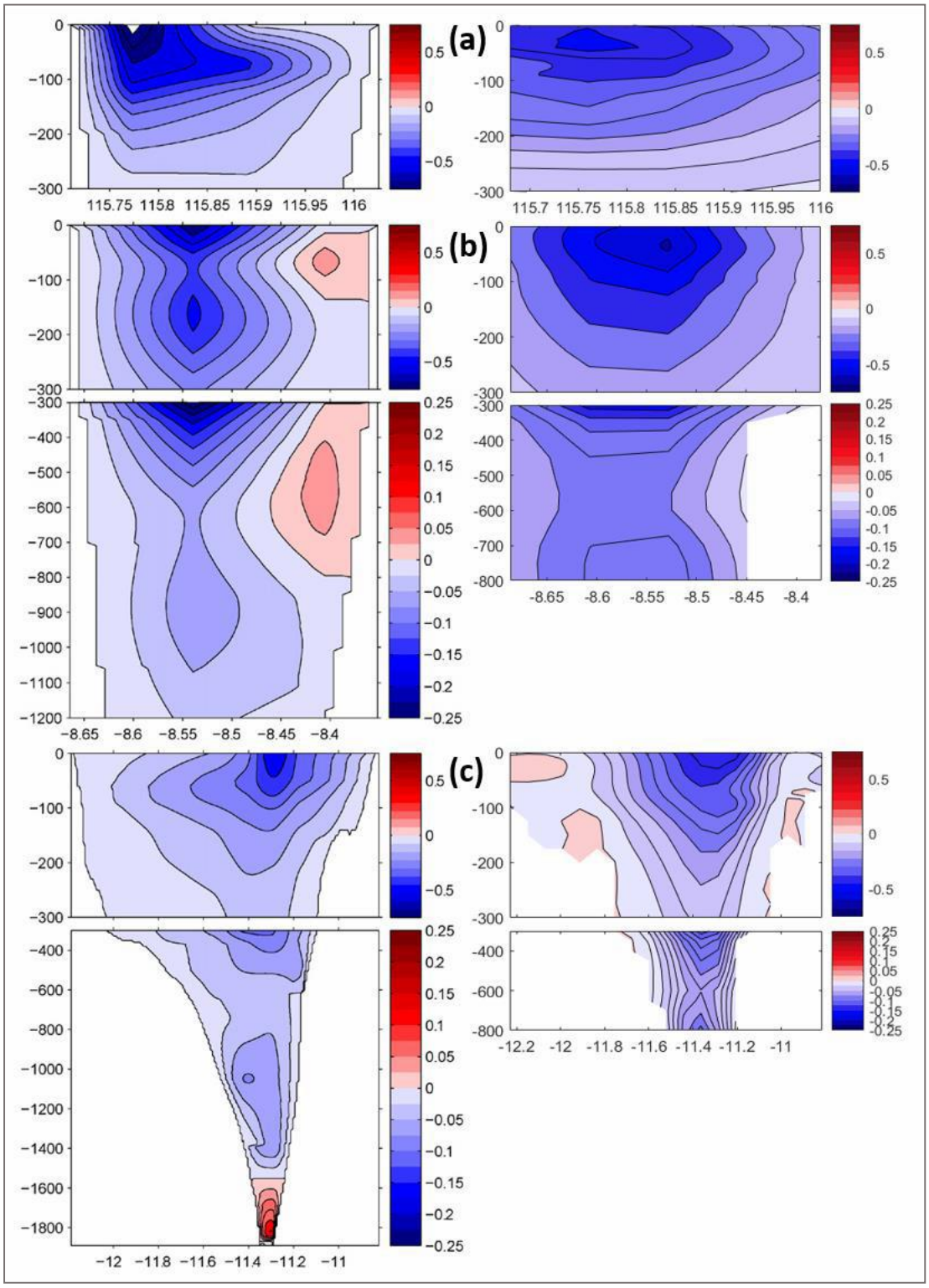

Fig. 5. Mean 2004–2006 along-strait velocity (cm/s) vs. depth for (a) Lombok Strait, (b) Ombai Strait and (c) Timor Passage from observations (left column) and the HYCOM reanalysis (right column). Note that negative values indicate flow into the Indian Ocean. The panels for observations are adapted from Metzger et al., 2010.

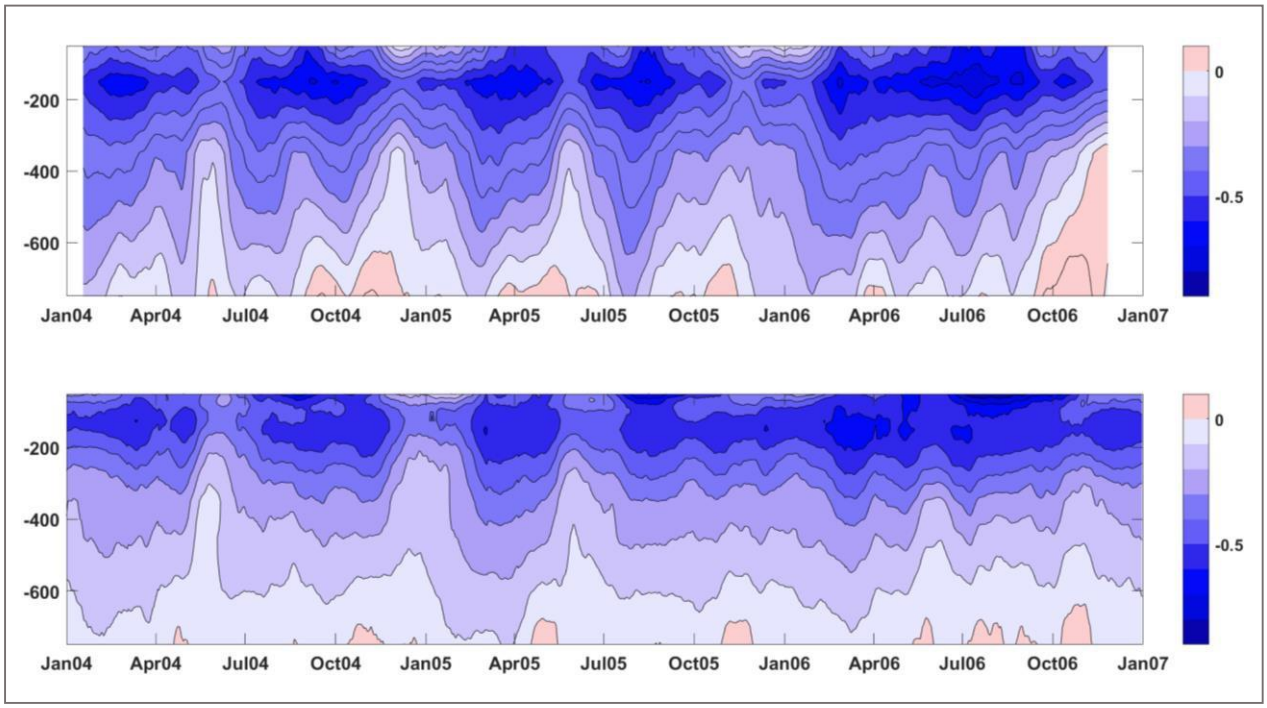

Fig. 6. Time series of along-strait velocity profile from INSTANT observations (top panel) and the HYCOM reanalysis (bottom panel).

The observational estimates should have some uncertainties, which may partly stem from the limited number of moorings across the straits. Fig. 7 shows the time series of the transport through the Makassar Strait estimated from INSTANT observations, the HYCOM reanalysis, and the estimates from the HYCOM reanalysis using the two nearest grid points to the mooring locations (calculated by the extrapolation method used in Gordon et al., 2008). Differences between the two estimates from the HYCOM reanalysis in transport (blue and red curves) sometimes exceed 1 Sv. These differences could be due to an intensification of the along-shore currents in the upper 200 m near the shelf break that is evident in the HYCOM reanalysis, which cannot be fully covered by the moorings (Fig. 8).

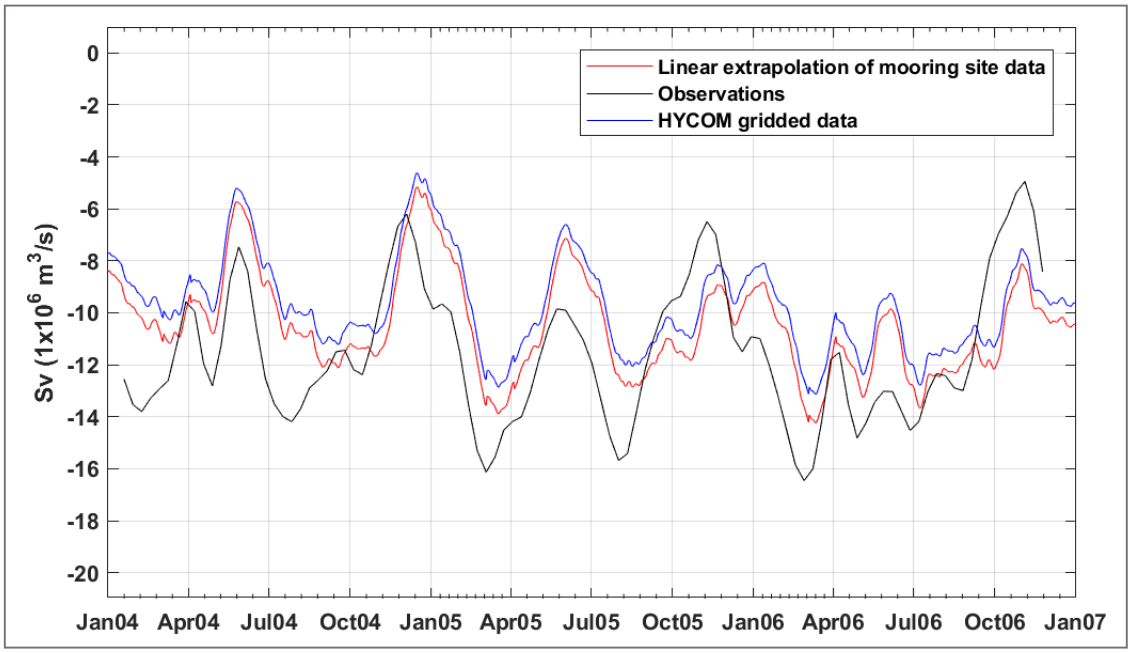

Fig. 7. Transport through the Makassar Strait estimated from observations (black line), from the HYCOM reanalysis (blue line) and estimates derived from only the velocity at the two grid points closest to the mooring locations in the HYCOM reanalysis by using the extrapolation method by Gordon et al., (2008) (red line).

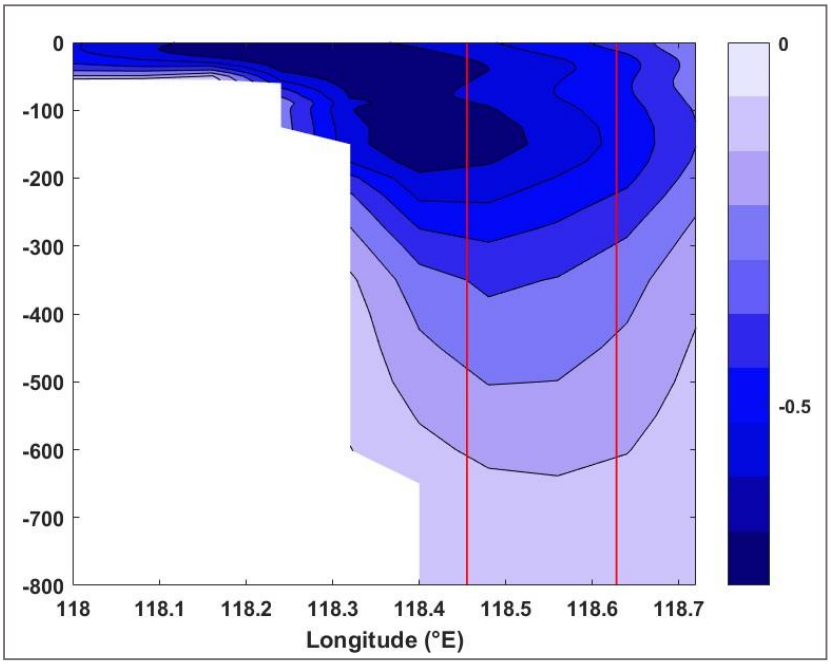

Fig. 8. Average along-strait velocity through the Makassar Strait (Labani Channel) during 2004-2006. The locations of INSTANT mooring observations are indicated by vertical red lines.

Since other data that include intraseasonal variability are not available in the Indonesian Seas, comparisons with the in-situ data for other regions in the tropical Indian Ocean are made to further validate the intraseasonal variability in the HYCOM reanalysis. Here, upper ocean current velocities are compared with DYNAMO and RAMA buoy measurements for the period of MJO onset in the central Indian Ocean. Fig. 9 shows the time series of near-surface zonal currents from observations (DYNAMO, solid line; RAMA, dotted line) and the HYCOM reanalysis (dashed line) for the period of mid-September 2011 to mid-January 2012. While there are differences in mean currents or long-term variations (Fig. 9a and Fig. 9b), intraseasonal variations associated with the MJO in the HYCOM analysis agree well with those of the observations (Fig. 9c and Fig. 9d). For example, the acceleration of the eastward jet on the equator in late November produced by the westerly winds associated with the MJO is well reproduced by the HYCOM reanalysis. Also, the agreement is very good for the first half of December 2011 and most of January 2012, including the rapid decay of equatorial jet in early January (Fig. 9c and Fig. 9d).

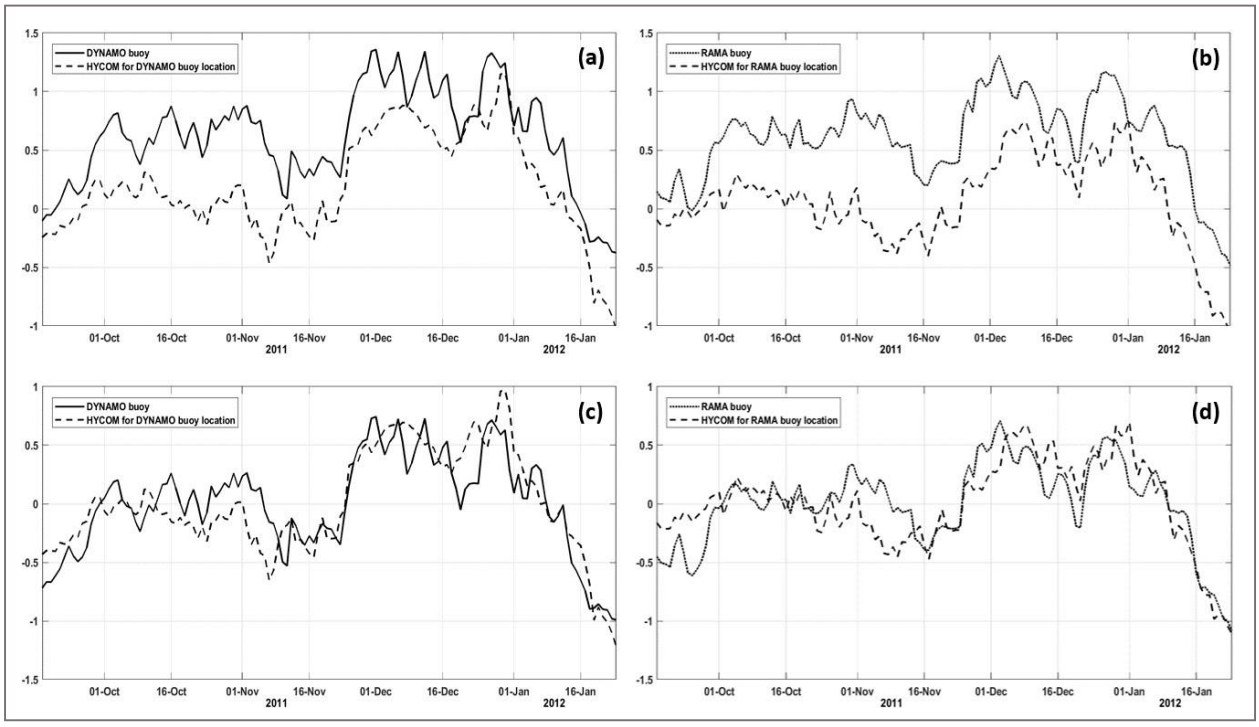

Fig. 9. (a) Daily surface zonal velocity (m/s) from the DYNAMO mooring at 0°, 79°E (solid) and from the HYCOM reanalysis at the DYNAMO's buoy location (dashed line), (b) same as (a) except from the RAMA mooring at 0°, 80.5°E (dotted line) and from the HYCOM reanalysis for the RAMA buoy location (dash line). (c) and (d), same as (a) and (b) but the mean values for each time series are subtracted.

Fig. 10 displays the time series of the vertical profile of zonal currents for the same period shown in Fig. 9. The profiles from the HYCOM reanalysis (top two panels of Fig. 10) agree fairly well with DYNAMO although some discrepancies are found. The model is able to reproduce well the vertical extent of the eastward jet and its intensification from the beginning of December 2011, in spite of its magnitude being smaller than the observed one. Also, the observations show a weak westward current at around 100 m after December 2011, which is also present in the reanalysis, although the currents are a little stronger.

The comparison of the reanalysis with RAMA buoy's data (Fig. 10 bottom two panels) also shows that the HYCOM reanalysis is capable of reproducing the eastward surface jet. After

December, the similar westward currents below the eastward jet is generated, which are well reproduced in the reanalysis, although it is a little stronger than observations.

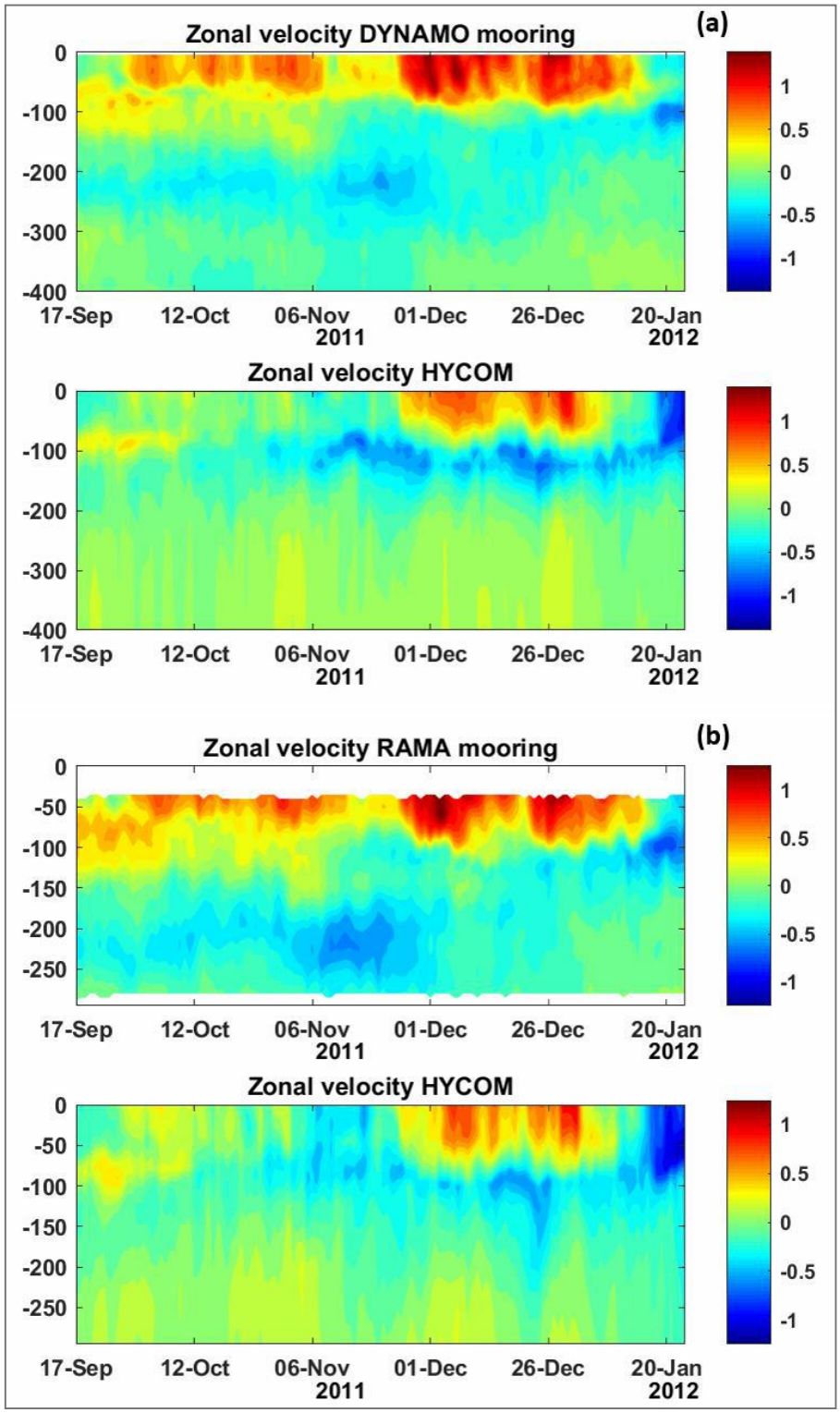

Fig. 10. (a) Vertical section of zonal velocity (m/s) at 0, 79°E (top) from the DYNAMO mooring and (bottom) from the HYCOM reanalysis. (b) Same as (a) from the RAMA mooring at 0°, 80.5°E (top) and from the HYCOM reanalysis (bottom). Note that the top two panels have different range of vertical axis than that of the bottom two panels.

A comparison between SSH derived from satellite altimeter (AVISO) and the HYCOM reanalysis is further performed for the period of the DYNAMO field campaign (Fig. 11). Due to the strong MJO event during DYNAMO, a strong eastward equatorial jet was generated, which produced a significant increase in SSH along the coast of Sumatra (e.g., Shinoda et al. 2017). The HYCOM reanalysis is able to reproduce the SSH anomalies near the Sumatra coast, as well as the negative anomalies in the central Indian Ocean around 5°S.

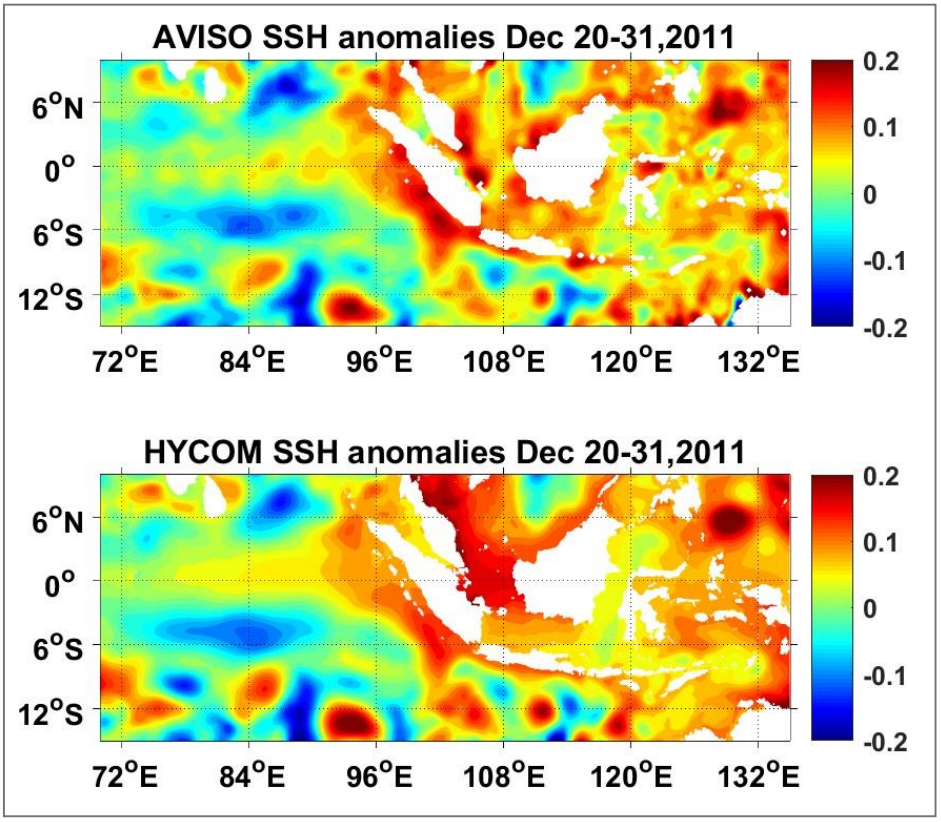

Fig. 11. (top) SSH anomalies (m) averaged for 20–31 December from AVISO satellite altimeter data. (bottom) Same as top but from HYCOM reanalysis.

The comparisons with observational data described above demonstrate that velocity and SSH fields in the HYCOM reanalysis including intraseasonal variations are sufficiently accurate for the further analysis, which will be described in the following sections.

3.2 MJO composites

3.2.a. ITF transport associated with the MJO

Based on the RMM index, 18 MJO events were detected for the 2004-2015 period. All of them except for two events are defined as those in which the index magnitude exceeds 1 for at least 30 consecutive days. The two exceptions are the events observed during DYNAMO (November-December 2011), which are widely discussed in previous studies (e.g., Gottschalck et al., 2013, Shinoda et al., 2013b, 2016, 2017, among others).

Composite transports of ITF through all major straits within the Indonesian Seas (Makassar, Lombok, Ombai Straits and Timor passage) and other narrow exit passages of ITF (Sunda and Sape Straits, Fig. 4) are calculated (Fig. 12). The sections used for the transport calculation are indicated in Fig. 4 as solid black lines. A significant reduction of the transport is found in all major straits during the MJO active phase over the MC (phase 4, 5 and 6), which is consistent with previous observational and modeling studies (e.g., Arief et al., 1996, Pujiana et al. 2013, Shinoda et al. 2016, Napitu et al., 2019). For all major ITF exit straits (except for Timor Passage), the reduction of the transport is around 2 Sv, which is similar to estimates from observations for Makassar Strait (Pujiana et al., 2013, Napitu et al., 2019). In addition to the reduction of ITF transport during the active phase, a significant enhancement of the ITF transport during the MJO suppressed phase over the MC (phase 1 and 2) is evident. The magnitude of the enhancement is comparable to that of the reduction during the active phase. For Lombok and Ombai Straits and Timor Passage, the enhancement of the transport is slightly smaller (~1 Sv) than the reduction. However, the amplitude (deviation from the mean) of the variation of the transport due to the MJO (~2 Sv) is comparable to their mean transport for both Lombok and Ombai Straits. For Makassar Strait, the enhancement of the transport during the suppressed phase is about 2 Sv,

which is also close to the reduction of the transport during the active phase. Hence the net effect of the MJO on the ITF transport is nearly zero, in which the reduction is nearly cancelled out by the enhancement. This can be verified on Table 2.

Strait / Passage	**Makassar**	**Sunda**	**Lombok**	**Sape**	**Ombai**	**Timor**
Av. anomalous transport (Sv)	0.03	-0.01	0.10	0.00	0.15	0.05

Table 2. Average anomalous transports (Sv) associated to the MJO in the MC major straits based on the composite of Fig. 12.

In addition to the prominent reduction during the MJO active phase and enhancement during the suppressed phase in all major straits, a variation of transport through other small passages such as Sunda and Sape strait is also significant (~0.5 and ~0.7 Sv respectively, Fig. 12). Given that the total transport for Sunda Strait varies from 0.24 ± 0.1 Sv in the boreal winter to –0.83 ± 0.2 Sv in the boreal summer (Susanto et al., 2016), the enhancement or reduction of the transport produced by the MJO could be more than twice of the total transport.

The fluctuation of ITF transport anomaly (Fig. 13a) and total transport (Fig. 13b) is further calculated by adding the transport anomaly and total transport values at all ITF exit passages (Lombok, Ombai, Sunda and Sape Straits and Timor Passage). The amplitude of the transport fluctuation due to intraseasonal variability is about 3-4.5 Sv (Fig. 13a, Fig. 13b), which is about 25 to 37% of the mean ITF transport. Note that the amplitude of the total transport fluctuation is not exactly the same as the amplitude of transport anomalies. This is because each MJO phase include the data from different seasons.

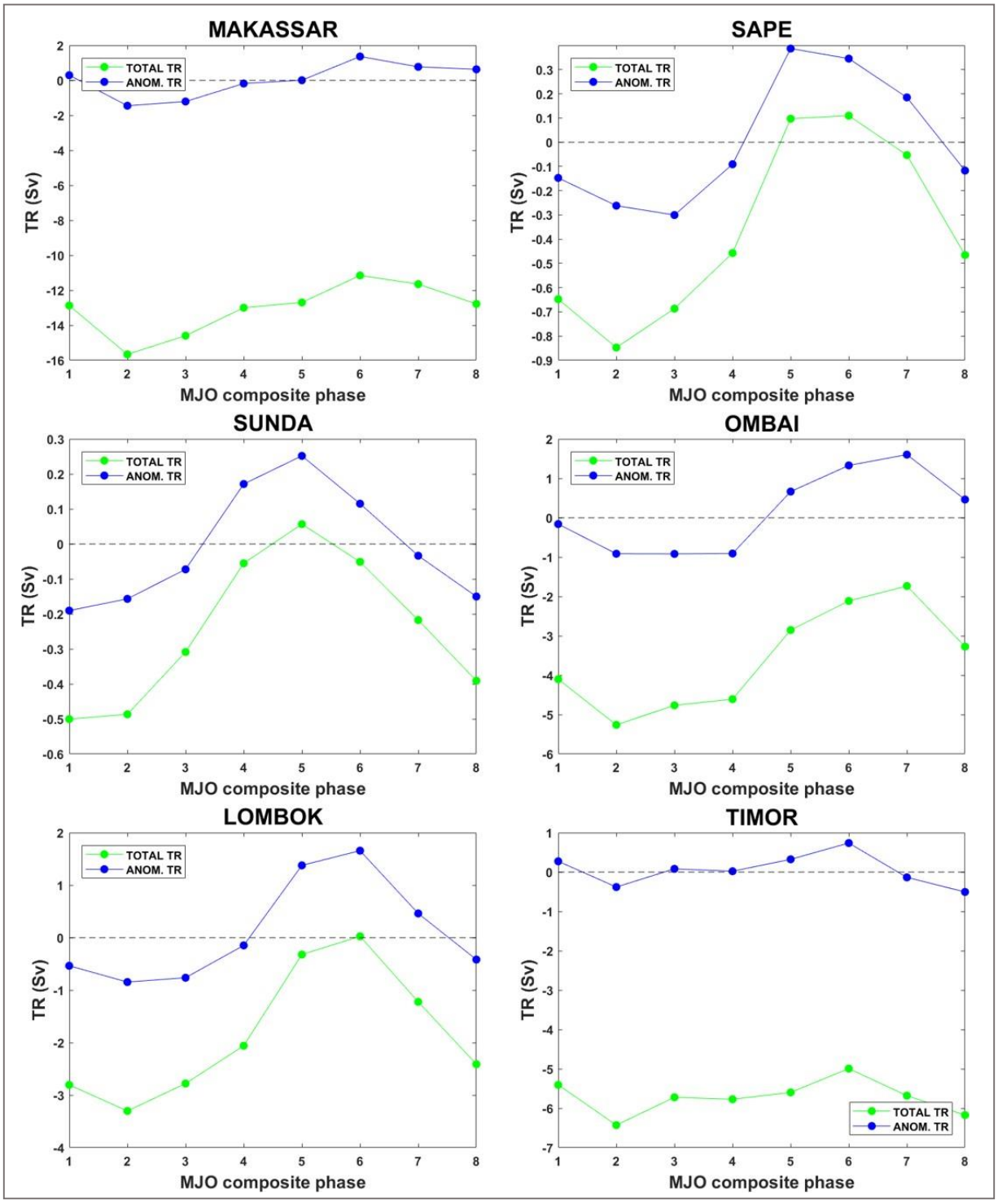

Fig. 12. MJO composite of total (green line) and anomalous (blue line) transport through Makassar Strait (upper left), Sunda strait (middle left), Lombok strait (bottom left), Sape strait (upper right), Ombai Strait (middle right) and Timor passage (lower right). See Fig. 4 for the locations of straits and passages.

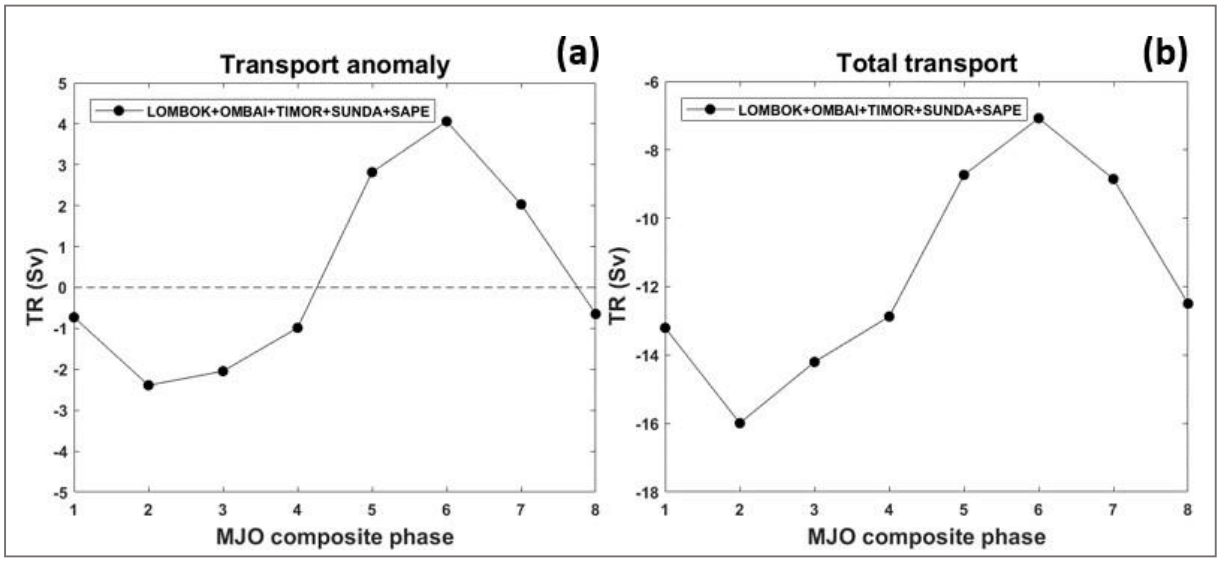

Fig. 13. MJO composite of anomalous (a) and total (b) transport for the summation of transport through all exit passages of ITF.

To further examine the vertical structure of current fluctuation, composite of the along-strait velocity across each strait is calculated. Fig. 14 shows the vertical section of the along-strait velocity across the Lombok Strait. The strong (> 0.2 m/s) anomalous southward currents (MJO phase 2) extends to only about 70 m depth while the northward anomalies (phase 6) extend all the way to about 150 m. Similar results are found for Ombai Strait and Timor Passage (not shown). In Ombai Strait, the difference between the vertical extent of current anomaly during the suppressed phase (~90 m) and active phase (~175 m) is similar to the one in Lombok Strait. For Timor passage, the difference is larger than that for Lombok (~35 m of vertical extent for the suppressed phase versus ~175 m for the active phase). These results suggest that the vertical motion near the coast changes the vertical extent of along-shore surface currents. To confirm the effect of vertical motion, the composite of the temperature along the same section in Lombok Strait is constructed (Fig. 15). The large cold anomalies around the thermocline depth (~100 m) during the suppressed phase suggest strong upwelling associated with negative SSH anomalies (described in the next

section), which can decrease the along-shore current vertical extent. Similarly, the warm anomalies around the thermocline depth indicate the downwelling during the active phase, which may cause the increase of the surface current vertical extent.

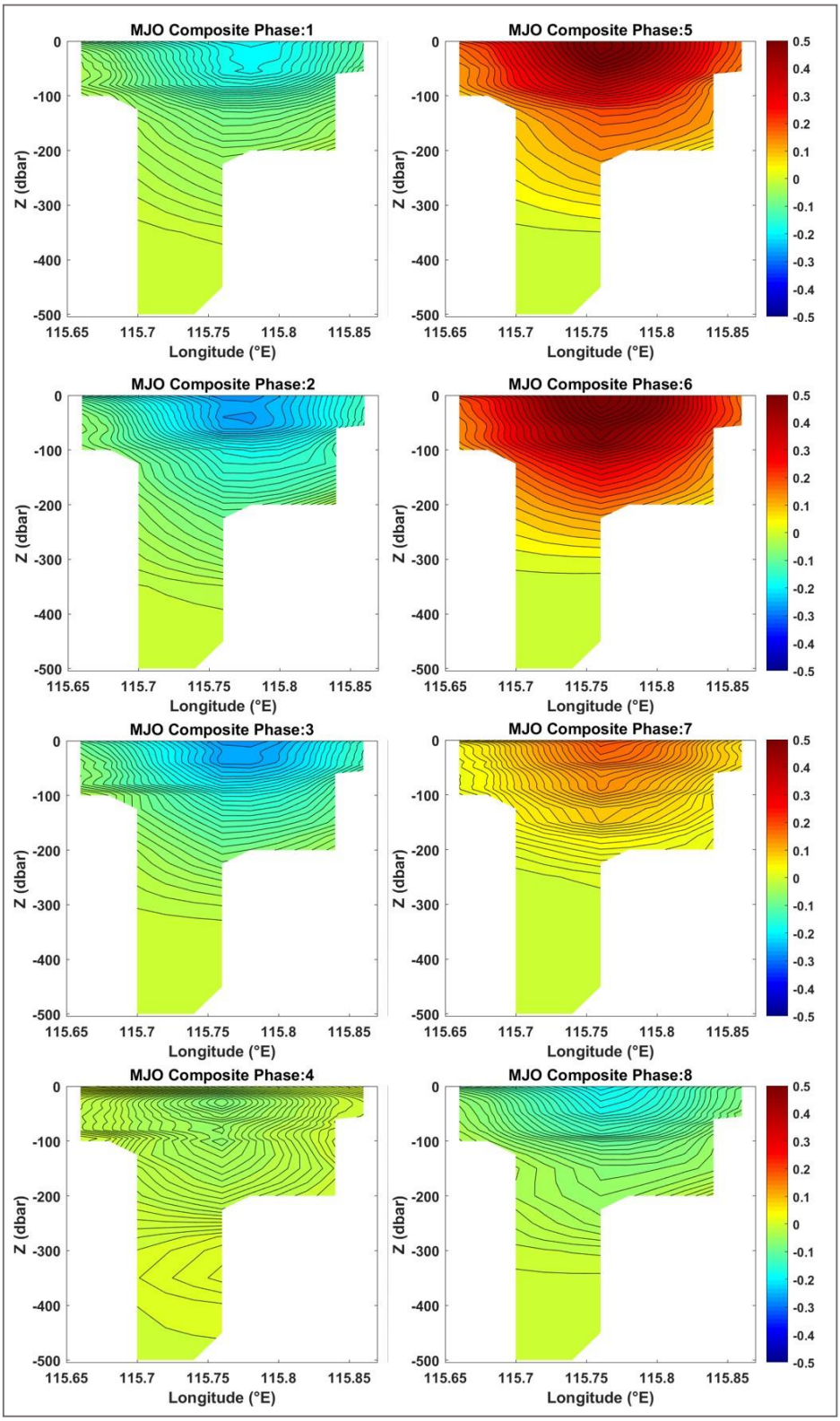

Fig. 14. MJO composite of along-strait velocity anomaly (m/s) across the Lombok strait. Positive values indicate northward currents.

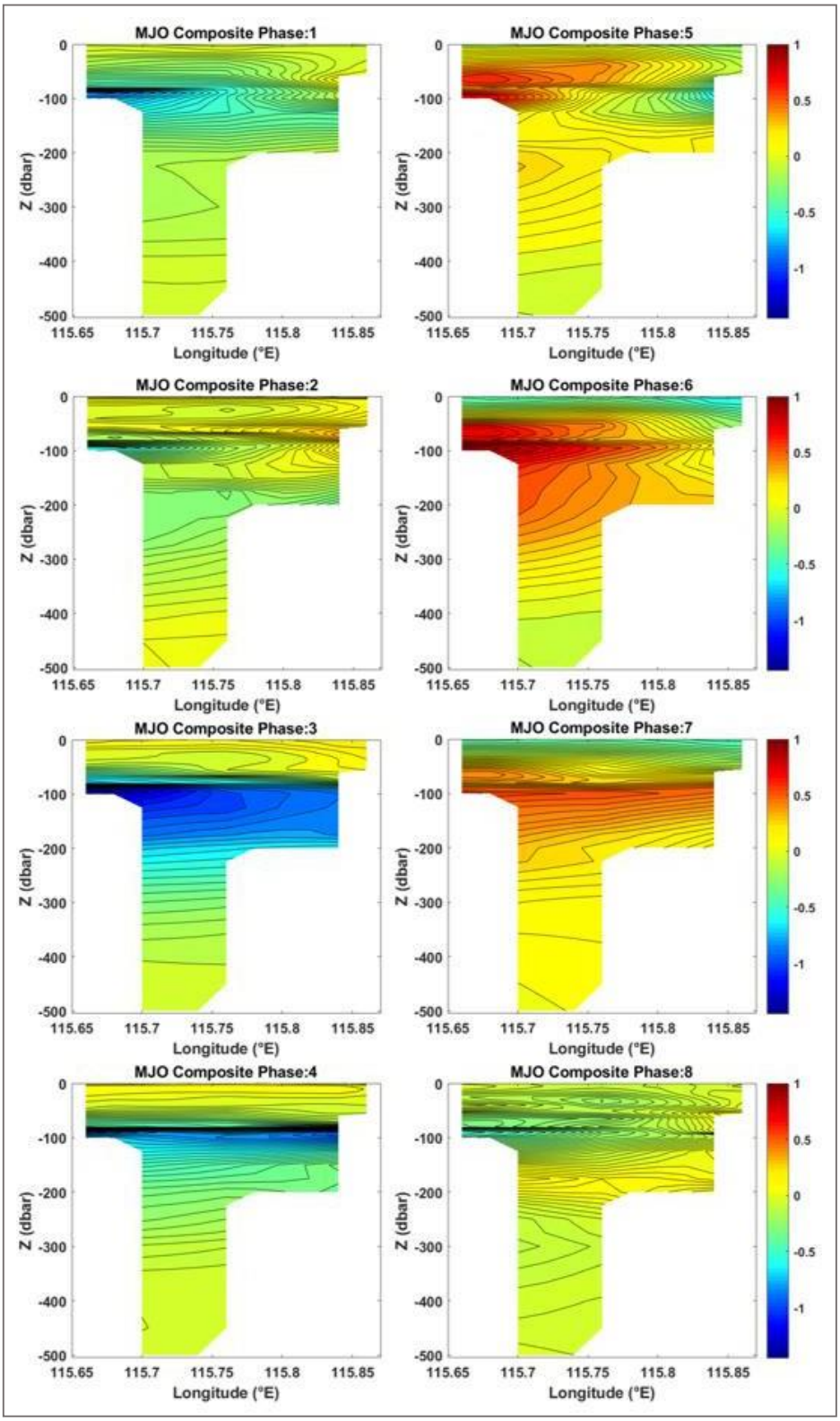

Fig. 15. MJO composite of temperature anomaly (°C) across the Lombok strait.

3.2.b. Large-scale ocean circulation around the Indonesian Seas

To compare MJO-associated oceanic variability with MJO-associated winds and atmospheric convection, composites of major atmospheric variables, OLR and surface winds, are constructed (Fig. 16). Consistent with previous MJO composite analyses (e.g., Pohl and Matthews 2007, Chattopadhyay et al., 2013, Zhang et al., 2019), negative OLR anomalies (intense convection) appear in the central Indian Ocean during phase 1 and 2 and the convection is centered over the MC around phase 4. Easterly wind anomalies are present over most of the MC for phases 8, 1 and 2 and they propagate eastward, followed by westerly and northwesterly (for the Southern Hemisphere) wind anomalies for phases 4, 5 and 6.

To describe the large-scale upper ocean variability associated with the MJO and to compare it with the transports through major straits, the composites of average ocean current velocity in the upper 150 m and SSH anomalies are computed (Fig. 17). During the MJO suppressed phase over the MC, negative SSH anomalies are present in most of the MC region, with maximum values along the Nusa Tenggara Islands. Along the southern coast of those islands, westward velocity anomalies associated to the SSH anomalies are found. In Makassar Strait, southward velocity anomalies are found, which is the same as the mean ITF direction. These southward anomalies reach the southern part of Indonesian Seas and exit mainly through Lombok but also through Sape Strait. Southward current anomalies in the western end of the Banda Sea (centered around 125°E, 5°S for MJO phase 2) exit the Indonesian Seas through Ombai Strait with values of around 0.2 m/s, and part of them might also exit through the Timor Passage. The southward anomalies present in the Banda Sea together with those found in Makassar Strait seem to be connected to the Pacific Ocean through the Celebes and Philippine Seas where westward current anomalies are found. The SSH and velocity anomalies shown on Fig. 17 are consistent with the enhancement of the ITF

transport described in the previous section, as the strong negative SSH anomalies south of the Nusa Tenggara Islands produce strong upwelling close to the exit passages. During the active phase, positive SSH anomalies are found over the entire MC region, with the maximum values along the Nusa Tenggara islands. On phase 5 of the MJO, the strong positive SSH anomalies along with the westward current anomalies to the south of the Nusa Tenggara islands penetrate into the Lombok Strait, producing very strong northward current anomalies, which are also found in Sape Strait. After penetrating the Indonesian Seas, those northward current anomalies travel westward into the Banda Sea, through the Flores Sea. During phases 6 and 7, the northward anomalies present in both Lombok and Sape Strait propagate northward to Makassar Strait all the way to the Celebes and Philippine Seas. The eastward current anomalies found in the south of the Nusa Tenggara archipelago during those phases propagate eastward along with the SSH positive anomalies, reaching Ombai Strait and entering the Flores Sea. At the same time, northward current anomalies found in the Banda Sea around 129°E, 5°S travel northward to the Ceram Sea where they are forced to the east by the topography, exiting to the north through the Halmahera and the Philippine Seas where they connect to the Pacific Ocean.

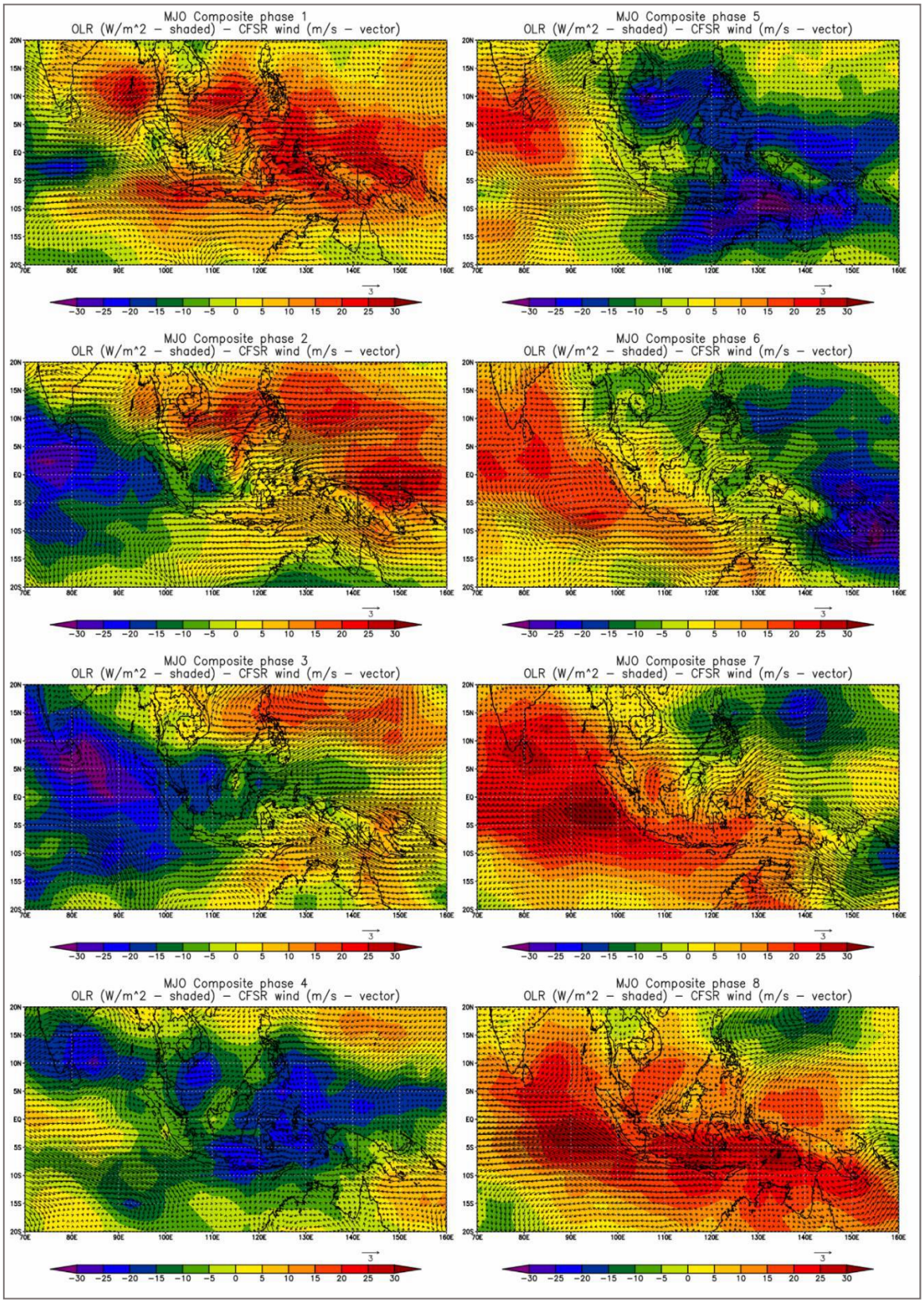

Fig. 16. MJO composite of OLR (W/m^2) and CFSR winds (m/s) at 10 m. height.

Fig. 18 shows composites of winds at 10 m height and wind speed for the MC area. During the MJO suppressed phase, anomalous easterly winds are evident over most of the MC region, with a maximum speed anomaly of about 1 to 2 m/s. Strong northeasterly wind anomalies are found over the Makassar Strait, which are favorable for causing the enhancement of the ITF. During the MJO active phase, the wind anomalies reverse their direction, which is westerly over most of the region and southwesterly over Lombok, Sape and Makassar Straits. The direction of the wind anomalies is also consistent with the reduction of the ITF transport during the active phase.

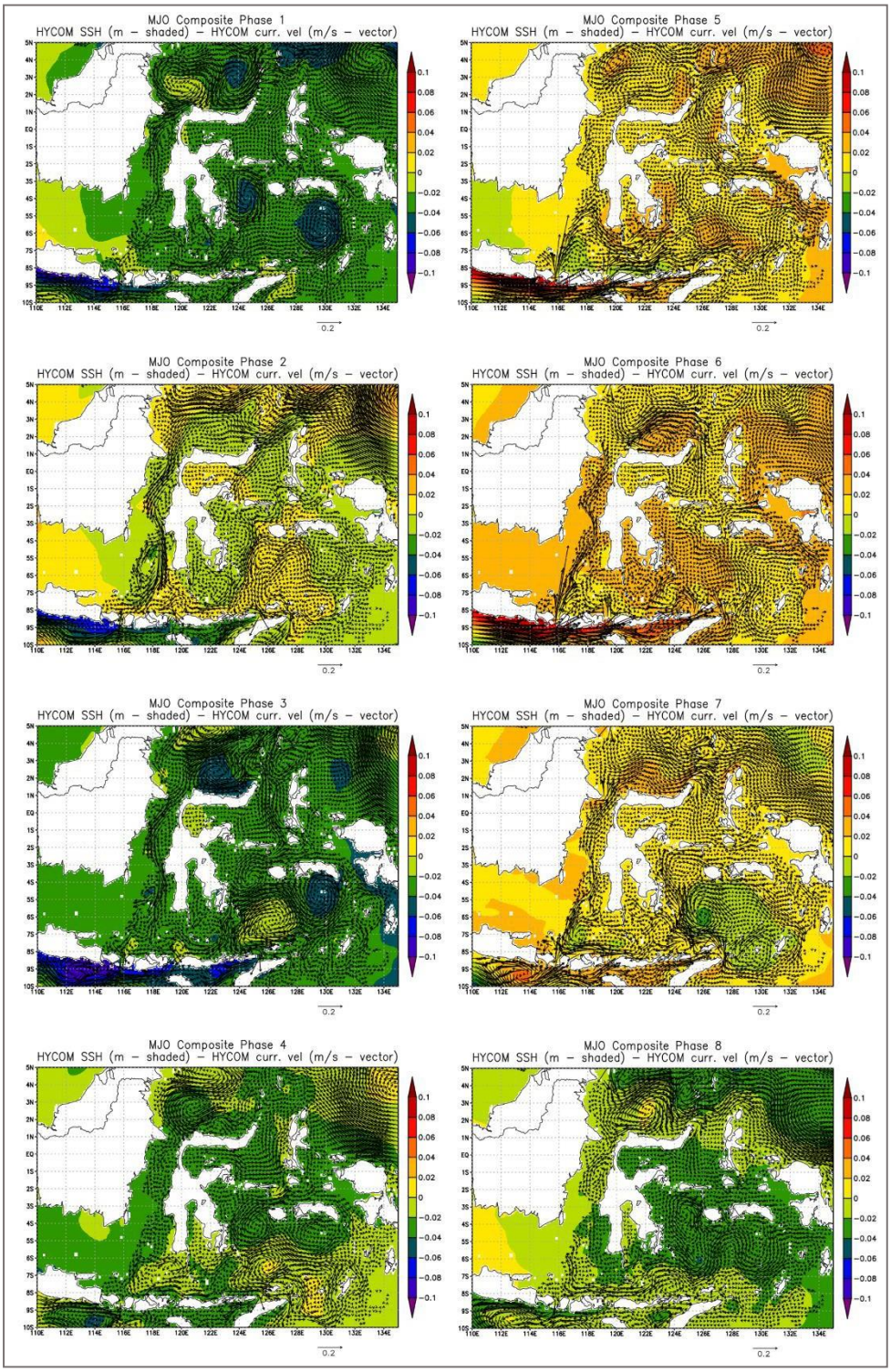

Fig. 17. MJO composite of upper-ocean (average over 0–150-m depths) velocity (m/s) and SSH anomalies (m) from the HYCOM reanalysis for the MC region.

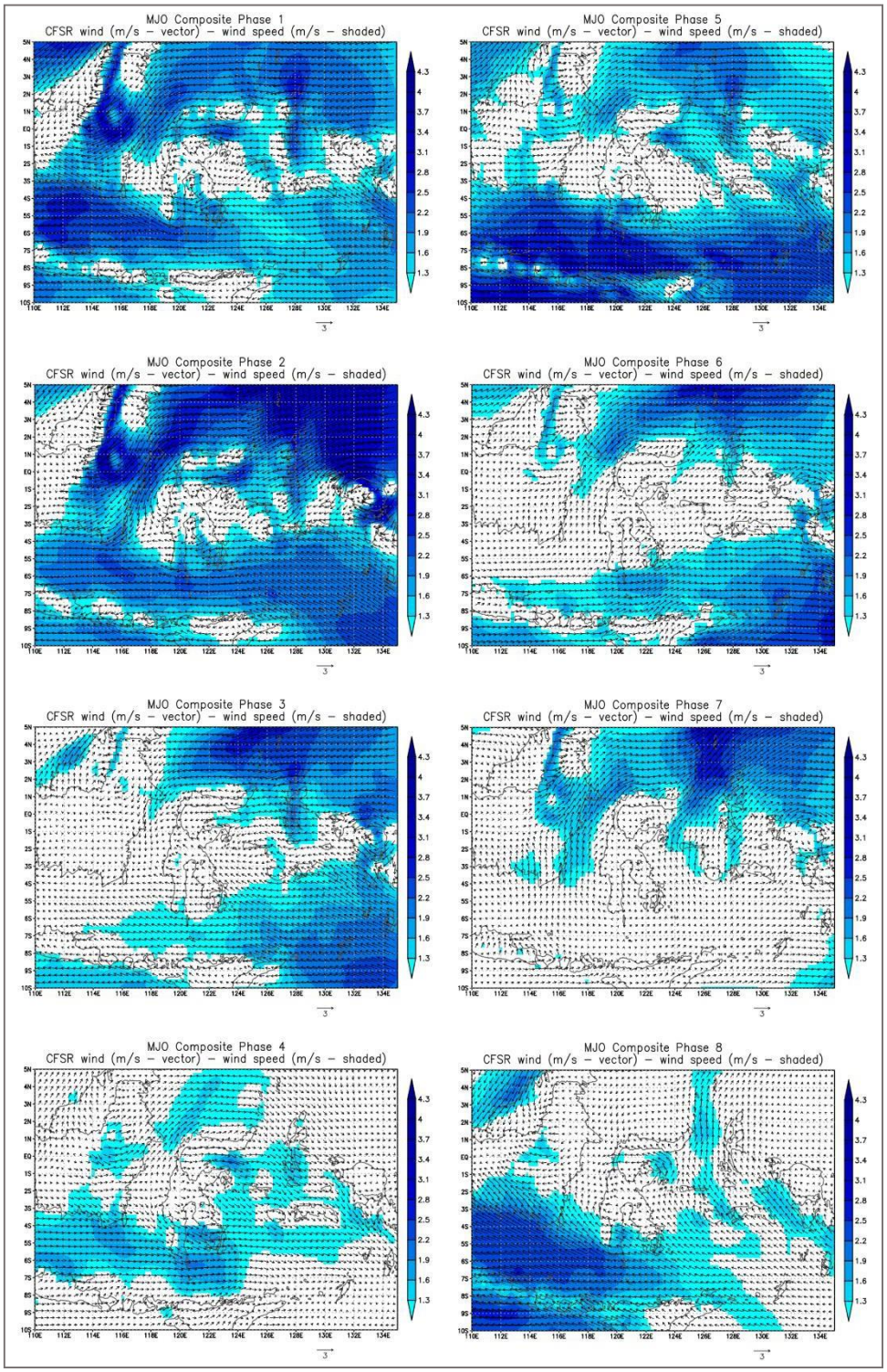

Fig. 18. Detail over the MC of the MJO composite of CFSR wind velocity (m/s) and speed (m/s) anomalies.

3.2.c. Influence of oceanic Kelvin waves generated by MJO forcing on ITF

The composites of average ocean current velocity in the upper 150 m and SSH anomalies are computed once again for a larger domain to examine the contribution of remotely forced ocean response to the MJO for the ITF transport variation (Fig. 19). During the MJO active phase over the MC (phases 4 and 5 of Fig. 19), when westerly winds are found in the equatorial Indian Ocean, eastward currents along the equator generate positive SSH anomalies at the eastern boundary. Then the anomalous SSH and southeastward along-shore currents propagate along the coast of Sumatra and Java islands. During the suppressed phase over the MC (phases 8 and 1 of Fig. 19), negative SSH anomalies with the magnitude and time evolution similar to those during the active phase are also present.

The same composite analysis is carried out using AVISO SSH data (Fig. 20) to validate the results obtained from the HYCOM reanalysis. The composite of SSH anomalies from AVISO is very similar to that from the HYCOM reanalysis, including the spatial distribution and magnitude. For example, for the MJO phase 1, both composites reveal negative SSH anomalies around the coast of Sumatra and Java with the magnitude of about -0.08 to -0.06 m, and during phase 5 the location of the positive SSH anomalies around the coast is nearly identical.

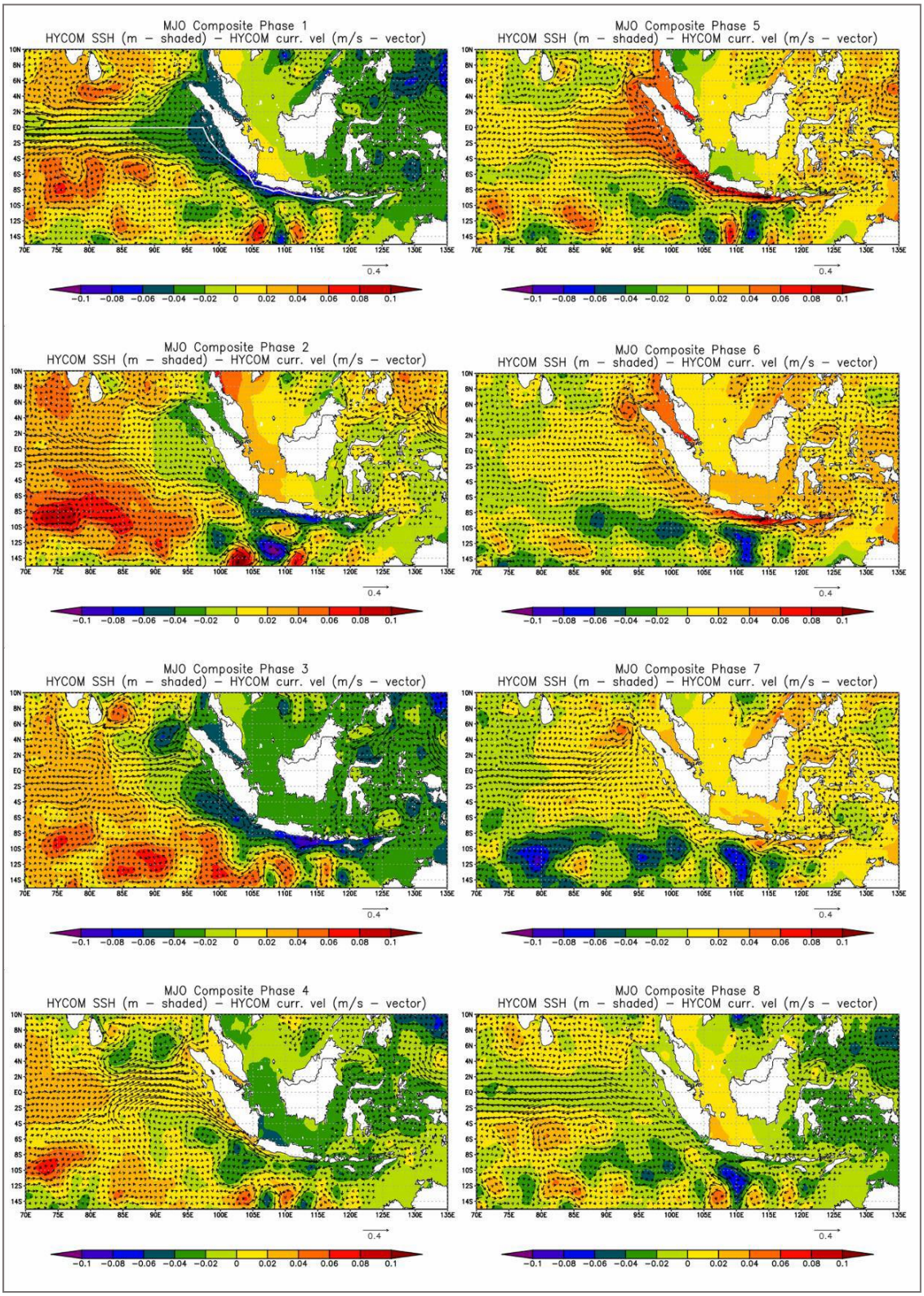

Fig. 19. Larger domain of the MJO composite of upper-ocean (average over 0–150-m depths) velocity (m/s) and SSH anomalies (m) from the HYCOM reanalysis.

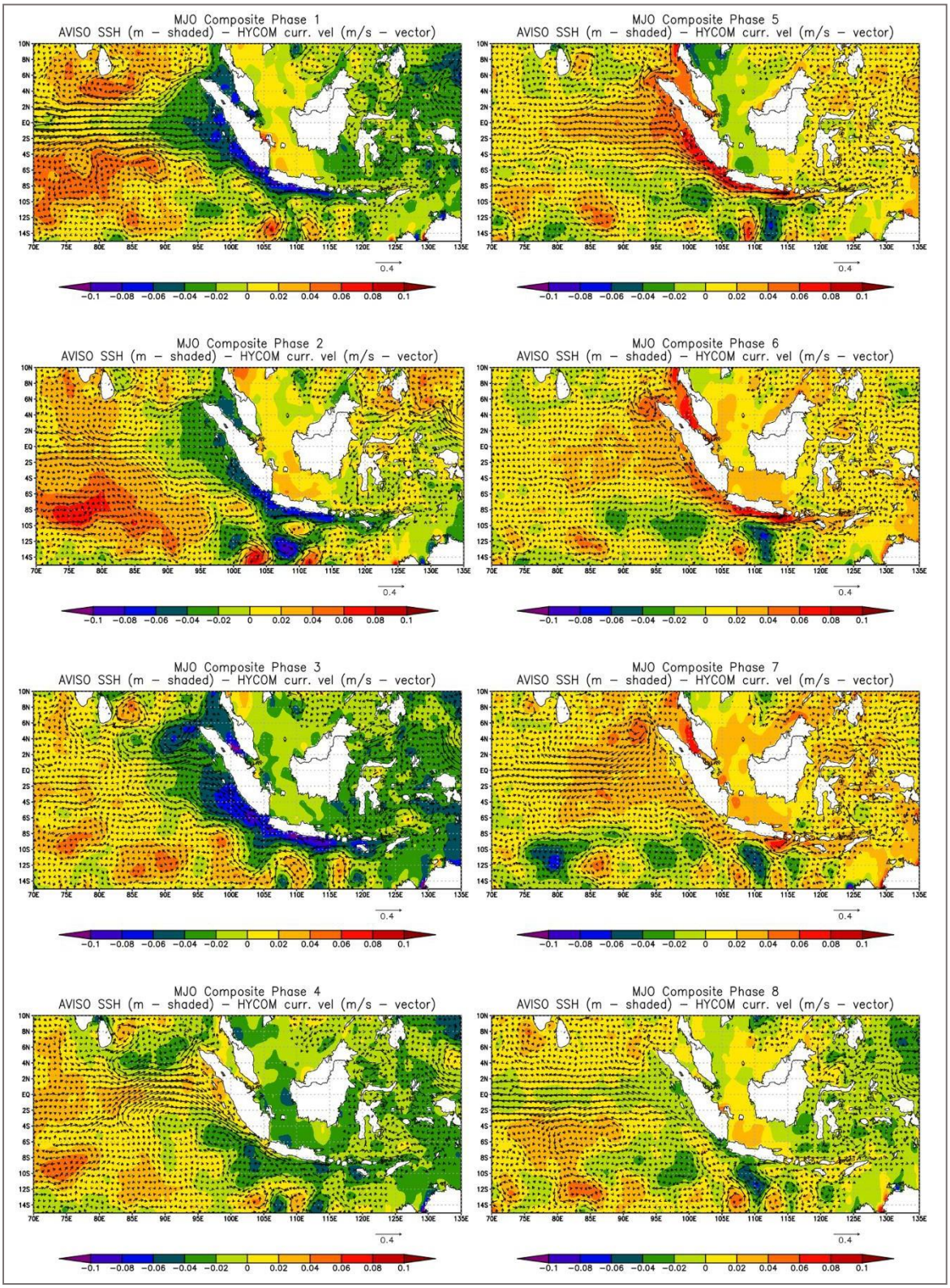

Fig. 20. MJO composite of upper-ocean (average over 0–150-m depths) velocity anomalies (m/s) from the HYCOM reanalysis and AVISO's SSH anomalies (m).

The propagation of SSH and upper ocean current anomalies during the MJO active phase shown in Fig. 19 and Fig. 20 appears to be consistent with MJO-induced coastal Kelvin waves from the central equatorial Indian Ocean, which are discussed in previous studies (e.g., Pujiana et al., 2013, Marshall and Hendon 2015, Shinoda et al. 2016, 2017).

To further examine the Kelvin wave propagation from the central Indian Ocean to Ombai Strait and Timor Passage, a Hovmöller diagram of composite SSH along the equatorial Indian Ocean and the coast of Sumatra and Java (lines shown in the top panel of Fig. 19 and Fig. 21) is constructed. (Fig. 22).

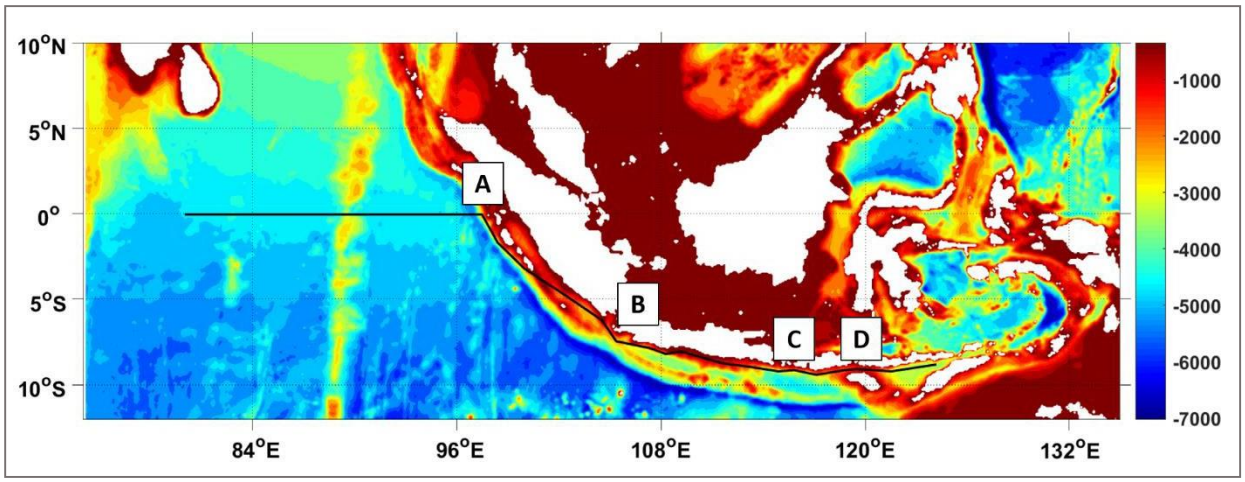

Fig. 21. Chosen path (black solid line) for the calculation of the Hovmöller diagram on top of 1/12° global HYCOM topography (m). The path is also featured on Fig. 19 upper left panel as a solid white line.

The propagation of positive SSH anomalies along the path (the line shown in Fig. 21) between phases 4 and 6 is clearly evident in SSH from both HYCOM reanalysis and AVISO. The phase speed (~2.9 m/s) is consistent with the first baroclinic mode Kelvin wave speed in this region (e.g., Drushka et al., 2010).

The propagation of negative SSH anomalies during phases 2 and 3 is not as clear as that in active phase in the composite. However, the propagation of the negative anomalies can be found for some of the MJO events, which will be discussed in Section 3.3.

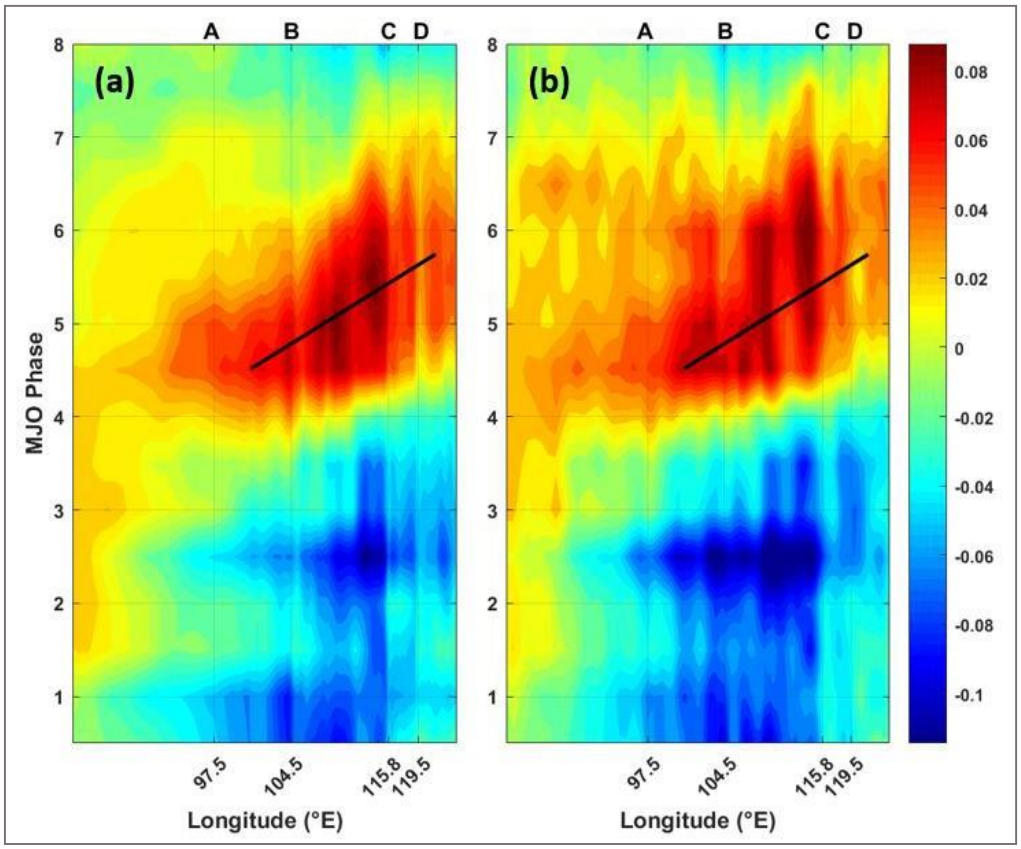

Fig. 22. Hovmöller diagram of SSH anomalies at different MJO phases from (a) HYCOM reanalysis and (b) AVISO. A, B, C, and D locations can be found on Fig. 21 and the black solid line indicates the phase line of ~2.9 m/s. A period of 65 days is used to calculate the phase speed.

3.3 Case study

To further evaluate the influence of the remote ocean response to the MJO on the upper ocean current variability, a case study for the period of the DYNAMO field campaign is carried out. During DYNAMO, three strong MJO events were observed (Gottschalck et al 2013, Shinoda et al., 2013b). While the intraseasonal variability of upper ocean currents during DYNAMO at

Makassar Strait and their mechanism have been discussed in a recent study (Shinoda et al. 2016), those in other areas including Sunda, Lombok and Ombai Straits and Timor Passage (Fig. 4) have not been examined so far. Fig. 23 shows the SSH and upper-ocean (average over 0–150-m depths) velocity anomalies during the period of suppressed phase and active phase of the MJO events observed in DYNAMO. During the suppressed phase, negative SSH anomalies and the associated anomalous currents are shown to propagate eastward from the Indian Ocean and along the coastline to the Nusa Tenggara Islands (Fig. 23). They are followed by positive SSH anomalies that also reach as far as Ombai Strait during the subsequent active phase. These variations of SSH and upper ocean currents during the MJO events observed in DYNAMO are consistent with the results of the composite analysis.

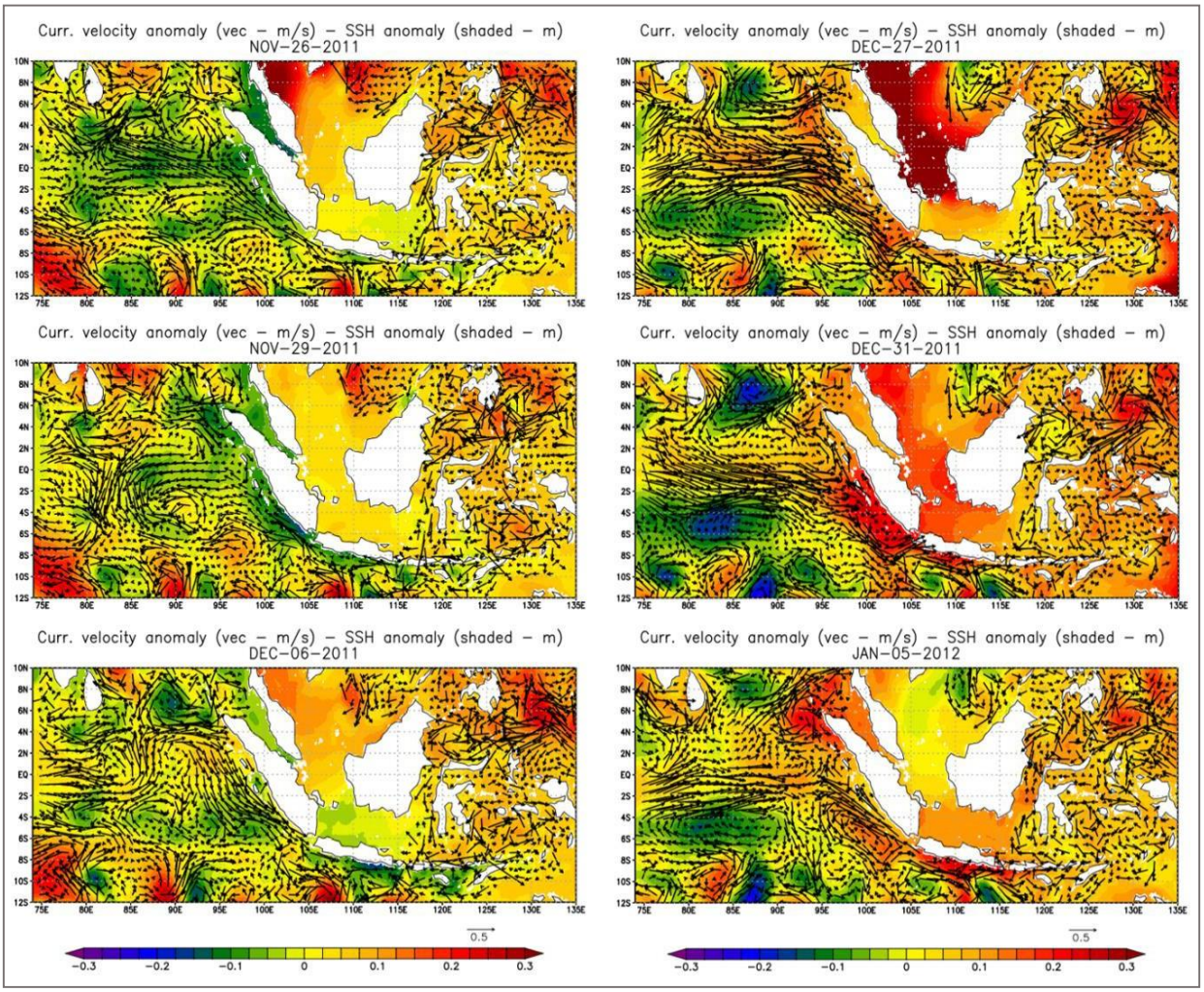

Fig. 23. SSH (shading; m) and upper-ocean (average over 0–150-m depths) velocity anomalies (vectors, m/s) for November 26, 29, December 06, 27, 31, 2011 and January 5, 2012 relative to the climatology for the 2004-2015 period from the HYCOM reanalysis.

Fig. 24 shows the Hovmöller diagram along the same path of Fig. 21 for HYCOM's SSH anomaly for the same dates as in Fig. 23. It is clear that both negative and positive anomalies propagate along the path with similar velocities, although the propagation for the negative anomalies is not clearly seen in the composite (Fig. 22). This suggests that the propagation of upwelling Kelvin waves during the suppressed phase occurs for some of the events, but it is not always observed during the MJO events used for the composite analysis. The eastward phase speed

for both negative and positive anomalies (~2.9 m/s) is consistent with that of the first baroclinic mode Kelvin wave.

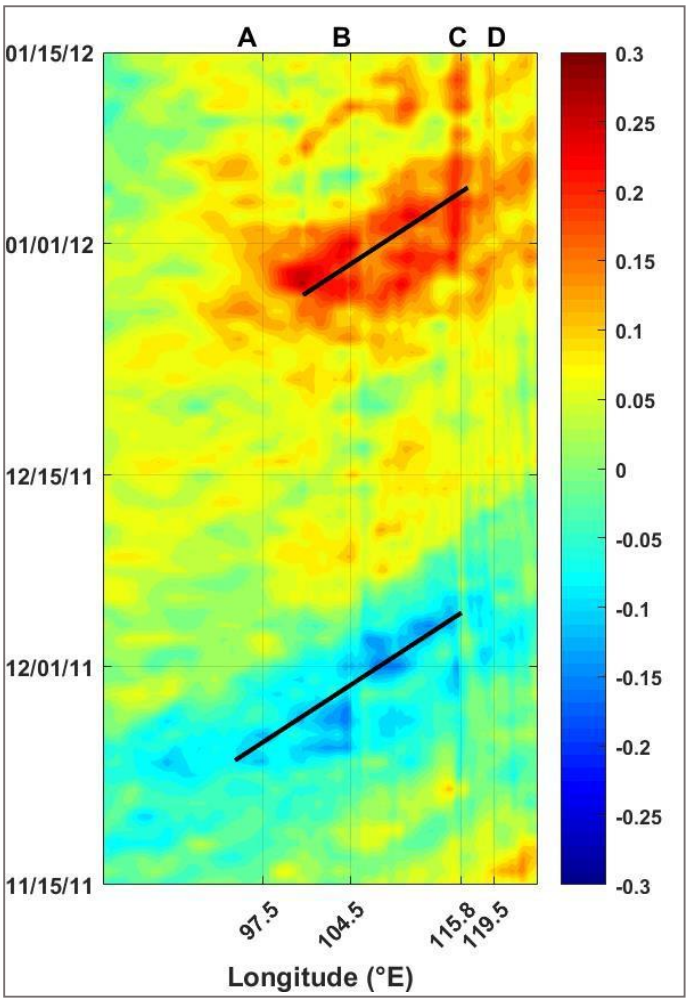

Fig. 24. Hovmöller diagram for the DYNAMO study case. A, B, C, and D locations can be found on Fig. 21. Black solid lines indicate the phase line of ~2.9 m/s.

To examine how the transport is modified during an MJO event, the transport through the Lombok Strait is calculated for the period of upwelling and downwelling Kelvin wave propagation (Fig. 25). Consistent with the composite transport (Fig. 12), an enhancement of the southward transport is found during the suppressed phase of the MJO when the negative SSH anomaly is

present (shown on the figure between light blue dashed lines). On the other hand, a reduction of the transport occurs during the active phase (between red dashed lines).

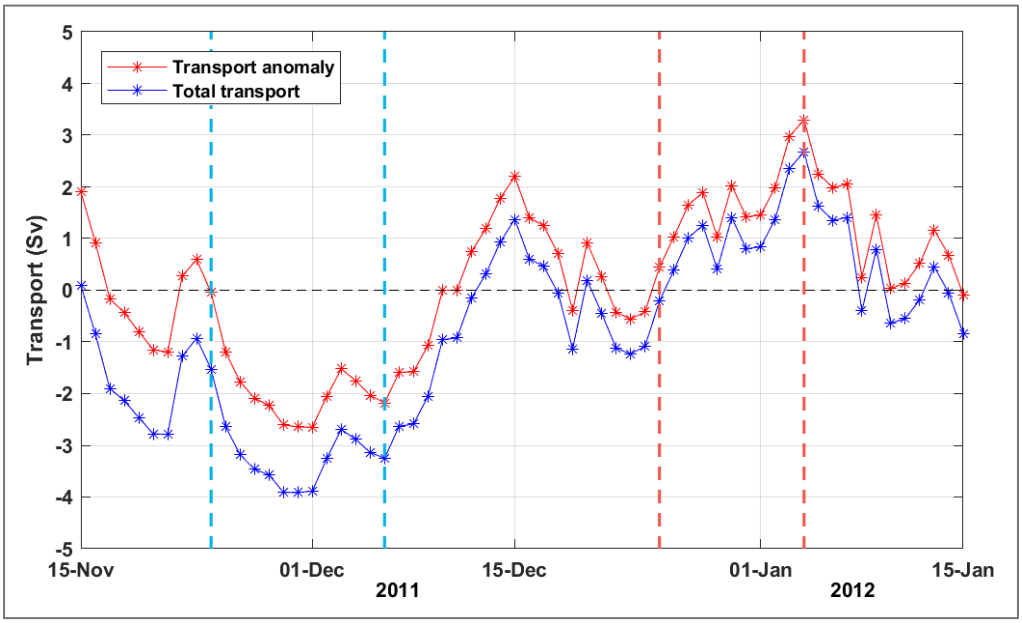

Fig. 25. Anomalous (red) and total (blue) transport through the Lombok strait during DYNAMO. Light blue dashed lines indicate the transport reduction period and the light red dashed lines, the transport enhancement period.

4. CONCLUSIONS

To quantify how the MJO influences the Indonesian Throughflow (ITF) transport through major straits over the Maritime Continent (MC) region, high-resolution ocean reanalysis (HYCOM reanalysis), satellite and in-situ observation data are analyzed. First, mean and intraseasonal variability in the ocean reanalysis are compared with the in-situ and satellite data. The mean transport through all major straits from observations are very similar to those calculated from the reanalysis. Also, the vertical structures of the mean currents in these straits agree well with observations. The variation of the along-strait velocity in Makassar Strait is well captured by the

HYCOM reanalysis including the intraseasonal variations based on the comparison with the INSTANT mooring data. It is noteworthy that the reanalysis shows an intensification of the along-strait mean current in Makassar near the shelf break that cannot be covered by the INSTANT moorings. The resulting error in the transport through Makassar could be estimated to be about 1 Sv. To further validate the intraseasonal variability in the HYCOM reanalysis, upper ocean currents in the central equatorial Indian Ocean are compared with DYNAMO and RAMA mooring data. It is found that the HYCOM reanalysis can adequately reproduce the intraseasonal variability of the upper ocean currents associated with the MJO. Also, the reanalysis is able to reproduce the large scale SSH variability associated with the MJO based on the comparison with the satellite altimeter data during DYNAMO.

To evaluate the impact of the MJO on the ITF transport, composite time series of transport through all major straits within the Indonesian Seas are calculated. A significant reduction of the transport during the active phase of the MJO over the MC is evident in all major straits. In addition, a large enhancement of the transport during the MJO suppressed phase is also clearly found in all straits, and the magnitude of the enhancement is comparable to that of the reduction. Hence the transport reduction during the active phase is almost canceled out by the enhancement during the suppressed phase and thus the net effect of the MJO on the ITF transport over its life cycle is nearly zero.

The vertical structure of the along-strait velocity in the exit passages is examined. The strong negative (southward) velocity anomalies in the Lombok Strait during the active phase extends to deeper areas than the positive (northward) anomalies during the suppressed phase. This difference is due to strong upwelling (downwelling) during the MJO suppressed (active) phase,

which is confirmed by the composite of temperature anomalies. The similar results were also found for Ombai Strait and Timor Passage.

Spatial distribution of composite oceanic variables in the HYCOM reanalysis is compared with the surface wind composite over the MC region. The results suggest that anomalous winds over the MC region contribute to the enhancement of the ITF transport during the MJO suppressed phase and the reduction during the active phase. During the active phase over the MC, the composite of SSH and upper ocean currents reveals that positive SSH anomalies and eastward currents propagate eastward along the coast of Java and Sumatra, and largely influence the ITF transport in major straits. The propagation speed of the positive SSH anomalies along the coast is consistent with the first baroclinic mode coastal Kelvin waves.

A case study is performed for the period of DYNAMO field campaign in fall/winter 2011 to confirm the influence of remote ocean response to the MJO on the ITF transport. SSH and upper ocean current anomalies during this period show the propagation of negative anomalies along the coast of Sumatra and Java during the suppressed phase of the MJO event followed by the propagation of positive anomalies during the active phase. A Hovmöller diagram confirms the propagation of the positive SSH anomalies whose phase speed is consistent with a first baroclinic mode of a Kelvin wave. Unlike the result of the composite analysis, the propagation of the negative SSH anomalies during the suppressed phase is also clearly evident during this particular event. This suggests that the propagation of upwelling Kelvin waves during the suppressed phase occurs for some of the events only, but it is not always observed. The enhancement and reduction of the transport in the Lombok Strait are evident during the DYNAMO MJO event which is also consistent with the composites.

REFERENCES

Arief, D., and Murray, S. P., 1996: Low-frequency fluctuations in the Indonesian throughflow through Lombok Strait, J. Geophys. Res., 101(C5), 12455–12464, doi:10.1029/96JC00051.

As-syakur, A.R., Osawa, T., Miura, F., Nuarsa, I.W., Ekayanti, N.W., Dharma, I.G.B.S., Adnyana, I.W.S., Arthana, I.W. and Tanaka, T., 2016: Maritime Continent rainfall variability during the TRMM era: The role of monsoon, topography and El Niño Modoki, Dynamics of Atmospheres and Oceans, Volume 75, Pages 58-77, ISSN 0377-0265, https://doi.org/10.1016/j.dynatmoce.2016.05.004

Bleck, R., 2002: An oceanic general circulation model framed in hybrid isopycnic-Cartesian coordinates. Ocean Modelling 4, 55–88.

Chattopadhyay, R., Vintzileos, A. and Zhang, C., 2013: A Description of the Madden-Julian Oscillation Based on a Self-Organizing Map. Journal of Climate. 26. 1716-1732. 10.1175/JCLI-D-12-00123.1.

Cummings, J. A., 2005: Prerational Multivariate Ocean data assimilation. Q. J. Meteorol. Soc. 131, 3583–3604.

Cummings, J.A. and Smedstad, O.M., 2013: Variational data assimilation for the global ocean. Park, S. K., Xu, L. (Eds), Data Assimilation for Atmospheric, Oceanic and Hydrologic Applications, vol. II. Springer-Verlag, Berlin, Heidelberg, pp. 303–343.

Drushka, K., Sprintall, J., Gille, S.T. and Brodjonegoro, I., 2010: Vertical Structure of Kelvin Waves in the Indonesian Throughflow Exit Passages. J. Phys. Oceanogr., 40, 1965–1987, https://doi.org/10.1175/2010JPO4380.1

Feng, J., T. Li, and W. Zhu, 2015: Propagating and Nonpropagating MJO Events over Maritime Continent. J. Climate, 28, 8430–8449, https://doi.org/10.1175/JCLI-D-15-0085.1

Gentilli, J., 1972: Thermal anomalies in the eastern Indian Ocean. Nature 238:93–95. https://doi.org/10.1038/physci238093a0

Gordon, A.L., Ma, S., Olson, D.B., Hacker, P., Ffield, A., Talley, L.D., Wilson, D. and Baringer, M., 1997: Advection and diffusion of Indonesian Throughflow water within the Indian Ocean South Equatorial Current, Geophys. Res. Lett., 24, 2573– 2576.

Gordon, A. L. and Susanto, R. D., 2001: Banda Sea surface-layer divergence, Ocean Dyn., 52, 2–10.

Gordon, A.L., Susanto, R.D., Ffield, A., Huber, B.A., Pronowo, W. and Wirasantosa, S., 2008: Makassar Strait throughflow, 2004 to 2006, Geophys. Res. Lett., 35, L24605, doi: 10.1029/2008GL036372.

Gottschalck, J., Roundy, P., Schreck, C., Vintzileos, A. and Zhang, C., 2013: Large-scale atmospheric and oceanic conditions during the 2011–12 DYNAMO field campaign. Mon. Wea. Rev., 141, 4173–4196, doi:10.1175/MWR-D-13-00022.1.

Guan, B., Lee, T., Halkides, D.J. and Waliser, D.E., 2014: Aquarius surface salinity and the Madden-Julian Oscillation: The role of salinity in surface layer density and potential energy, Geophys. Res. Lett., 41, 2858–2869, doi:10.1002/2014GL059704.

Han, W., 2005: Origins and dynamics of the 90-day and 30–60-day variations in the equatorial Indian Ocean. J. Phys. Oceanogr., 35, 708–728, doi:10.1175/JPO2725.1.

Keenan, T., Rutledge, S., Carbone, R., Wilson, J., Takahashi, T., May, P., Tapper, N., Platt, M., Hacker, J., Sekelsky, S., Moncrieff, M. and Saito, K., 2000: The Maritime Continent Thunderstorm Experiment (MCTEX): Overview and Some Results. Bulletin of the American Meteorological Society. 81. 2433-2455. 10.1175/1520-0477(2000)081<2433:TMCTEM>2.3.CO;2.

Kim, D., Kim, H., and Lee, M.I., 2017: Why does the MJO detour the Maritime Continent during austral summer?, Geophys. Res. Lett., 44, 2579– 2587, doi:10.1002/2017GL072643.

Koch-Larrouy, A., Madec, G., Iudicone, D., Atmadipoera, A. and Molcard, R., 2008: Physical processes contributing to the water mass transformation of the Indonesian Throughflow, Ocean Dyn., 58(3), 275–288.

Lau, K., and Chan, P.H., 1983a: Short-term climate variability and atmospheric teleconnections from satellite-observed outgoing longwave radiation. Part I: Simultaneous relationships. J. Atmos. Sci, 40, 2735–2750.

Lau, K., Chang, C., and Chan, P.H., 1983b: Short-Term Planetary-Scale Interactions over the Tropics and Midlatitudes. Part II: Winter-MONEX Period. Mon. Wea. Rev., 111, 1372–1388, https://doi.org/10.1175/1520-0493(1983)111<1372:STPSIO>2.0.CO;2

Liebmann, B. and Smith, C.A., 2006: Description of a Complete (Interpolated) Outgoing Longwave Radiation Dataset. Bulletin of the American Meteorological Society, 77, 1275-1277.

Liu Q, Feng M, Wang D, Wijffels S (2015) Interannual variability of the Indonesian throughflow transport: a revisit based on 30 year expendable bathythermograph data. J Geophys Res Oceans 120:8270–8282. https://doi.org/10.1002/2015JC011351

Madden, R.A. and Julian, P.R., 1971: Detection of a 40–50 Day Oscillation in the Zonal Wind in the Tropical Pacific. J. Atmos. Sci., 28, 702–708, https://doi.org/10.1175/1520-0469(1971)028<0702:DOADOI>2.0.CO;2

Madden, R.A. and Julian, P.R., 1972: Description of Global-Scale Circulation Cells in the Tropics with a 40–50 Day Period. J. Atmos. Sci., 29, 1109–1123, https://doi.org/10.1175/1520-0469(1972)029<1109:DOGSCC>2.0.CO;2

Marshall, A. G., and Hendon, H. H., 2015: Subseasonal prediction of Australian summer monsoon anomalies, Geophys. Res. Lett., 42, 10,913–10,919, doi:10.1002/ 2015GL067086.

Masumoto, Y., 2002: Journal of Oceanography 58: 175. https://doi.org/10.1023/A:1015889004089

McBride, J.L., 1998: Indonesia, Papua New Guinea, and tropical Australia. The Southern Hemisphere summer monsoon. Meteorology of the Southern Hemisphere, Meteor. Monogr., No. 49, Amer. Meteor. Soc., 89–99.

McPhaden, M.J., Meyers, G., Kentaro, A., Masumoto, Y., Murty, V.S.N., & Ravichandran, M., Syamsudin, F., Vialard, J., Yu, L. and Yu, W., 2009: RAMA The Research Moored Array for African-Asian-Australian Monsoon Analysis and Prediction. Bulletin of the American Meteorological Society. 90. 0.1175/2008BAMS2608.1.

Meehl, G.A., 1987: The annual cycle and interannual variability in the tropical Pacific and Indian Ocean regions. Mon. Wea. Rev., 115, 27–50.

Metzger, E.J., Hurlburt, H.E., Xu, X., Shriver, J.F., Gordon, A.L., Sprintall, J., Susanto, R.D., van Aken, H.M., 2010: Simulated and observed circulation in the Indonesian Seas: 1 / 12°global HYCOM and the INSTANT observations. Dynamics of Atmospheres and Oceans. 50:275-300.

Meyers, G., Bailey, R.J., Worby, A.P., 1995: Geostrophic transport of Indonesian throughflow, Deep Sea Research Part I: Oceanographic Research Papers, Volume 42, Issue 7, Pages 1163-1174, ISSN 0967-0637, https://doi.org/10.1016/0967-0637(95)00037-7.

Meyers, G., 1996: Variation of Indonesian throughflow and the El Niño-Southern Oscillation, J. Geophys. Res., 101 (C5), 12255– 12263, doi:10.1029/95JC03729.

Moore, D. W. and McCreary, J. P., 1990: Excitation of intermediate frequency equatorial waves at a western ocean boundary: With application to observations from the western Indian Ocean. J. Geophys. Res., 95, 5219–5231, doi:10.1029/JC095iC04p05219.

Moum, J.N., de Szoeke, S.P., Smyth, W.D., Edson, J.B., DeWitt, H.L., Moulin, A.J., Thompson, E.J., Zappa, C.J., Rutledge, S.A., Johnson, R.H. and Fairall, C.W., 2014: Air–Sea Interactions from Westerly Wind Bursts During the November 2011 MJO in the Indian Ocean. Bull. Amer. Meteor. Soc., 95, 1185–1199, https://doi.org/10.1175/BAMS-D-12-00225.1

Napitu, A. M., 2017: Response of the Indonesian Seas and its potential feedback to the Madden Julian Oscillation (Doctoral Thesis). Retrieved from Columbia University Libraries.

Napitu, A. M., Pujiana, K., and Gordon, A. L., 2019: The Madden-Julian Oscillation's impact on the Makassar Strait surface layer transport. Journal of Geophysical Research: Oceans, 124, 3538–3550. https://doi.org/10.1029/2018JC014729

National Center for Atmospheric Research Staff (Eds), 2016: The Climate Data Guide: AVISO: Satellite derived Sea Surface Height above Geoid. Retrieved from https://climatedataguide.ucar.edu/climate-data/aviso-satellite-derived-sea-surface-height-above-geoid.

Neale, R. and Slingo, J., 2003: The Maritime Continent and Its Role in the Global Climate: A GCM Study. J. Climate, 16, 834–848, https://doi.org/10.1175/1520-0442(2003)016<0834:TMCAIR>2.0.CO;2

Philander, S.G.H., 1985: El Niño and La Niña. J. Atmos. Sci., 42, 652–662.

Pohl, B. and Matthews, A., 2007: Observed Changes in the Lifetime and Amplitude of the Madden Julian Oscillation Associated with Interannual ENSO Sea Surface Temperature Anomalies. Journal of Climate. 20. 2659-. 10.1175/JCLI4230.1.

Pujiana, K., Gordon, A.L. and Sprintall, J., 2013: Intraseasonal Kelvin wave in Makassar Strait, J. Geophys. Res. Oceans, 118, 2023– 2034, doi:10.1002/jgrc.20069.

Qian, J., 2008: Why precipitation is mostly concentrated over islands in the Maritime Continent. J. Atmos. Sci., 65, 1428–1441, https://doi.org/10.1175/2007JAS2422.1

Qiu, B., Mao, M. and Kashino, Y., 1999: Intraseasonal variability in the Indo-Pacific Throughflow and the regions surrounding the Indonesian Seas. J. Phys. Oceanogr., 29, 1599–1618.

Ramage, C.S., 1968: Role of a tropical "maritime continent" in the atmospheric circulation. Mon. Wea. Rev., 96, 365–370.

Rejeki, H.A., Munasik, Kunarso, 2017: IOP Conf. Ser.: Earth Environ. Sci. 55 012066.

Saha, S., Moorthi, S., Pan, H., Wu, X., Wang, J., Nadiga, S., Tripp, P., Kistler, R., Woollen, J., Behringer, D., Liu, H., Stokes, D., Grumbine, R., Gayno, G., Wang, J., Hou, Y., Chuang, H., Juang, H.H., Sela, J., Iredell, M., Treadon, R., Kleist, D., Van Delst, P., Keyser, D., Derber, J., Ek, M., Meng, J., Wei, H., Yang, R., Lord, S., van den Dool, H., Kumar, A., Wang, W., Long, C., Chelliah, M., Xue, Y., Huang, B., Schemm, J., Ebisuzaki, W., Lin, R., Xie, P., Chen, M., Zhou, S., Higgins, W., Zou, C., Liu, Q., Chen, Y., Han, Y., Cucurull, L., Reynolds, R.W., Rutledge, G. and Goldberg, M., 2010: The NCEP Climate Forecast System Reanalysis. Bull. Amer. Meteor. Soc., 91, 1015–1058, https://doi.org/10.1175/2010BAMS3001.1

Saha, S., Moorthi, S., Wu, X., Wang, J., Nadiga, S., Tripp, P., Behringer, D., Hou, Y., Chuang, H., Iredell, M., Ek, M., Meng, J., Yang, R., Mendez, M.P., van den Dool, H., Zhang, Q., Wang, W., Chen, M. and Becker, E., 2014: The NCEP Climate Forecast System Version 2. J. Climate, 27, 2185–2208, https://doi.org/10.1175/JCLI-D-12-00823.1

Saji, N.H., Goswami, B.N., Vinayachandran, P.N., and Yamagata, T., 1999: A dipole mode in the tropical Indian Ocean. Nature, 401(6751), 360-363.

Schiller, A., Wijffels, S.E., Sprintall, J., Molcard, R. and Oke, P., 2010: Pathways of intraseasonal variability in the Indonesian Throughflow region. Dynamics of Atmospheres and Oceans. 50. 174-200. 10.1016/j.dynatmoce.2010.02.003.

Sen Gupta, A., Ganachaud, A., McGregor, S., Brown, J. N. and Muir, L., 2012: Drivers of the projected changes to the Pacific Ocean equatorial circulation, Geophys. Res. Lett., 39, L09605, doi:10.1029/2012GL051447.

Shinoda, T., Jensen, T.G., Flatau, M., Chen S., Han, W. and Wang, C., 2013b: Large-scale oceanic variability associated with the Madden–Julian oscillation during the CINDY/DYNAMO field campaign from satellite observations. Remote Sens., 5, 2072–2092, doi:10.3390/rs5052072.

Shinoda, T., Han, W., Jensen, T.G., Zamudio, L., Metzger, E.J. and Lien, R., 2016: Impact of the Madden–Julian Oscillation on the Indonesian Throughflow in the Makassar Strait during

the CINDY/DYNAMO Field Campaign. J. Climate, 29, 6085–6108, https://doi.org/10.1175/JCLI-D-15-0711.1

Shinoda, T., Han, W., Zamudio, L., Lien, R.-C., Katsumata, M., 2017: Remote Ocean Response to the Madden–Julian Oscillation during the DYNAMO Field Campaign: Impact on Somali Current System and the Seychelles–Chagos Thermocline Ridge. Atmosphere, 8, 171.

Song, Q., A. L. Gordon, and M. Visbeck (2004), Spreading of the Indonesian throughflow in the Indian Ocean, J. Phys. Oceanogr., 34, 772– 779.

Sprintall, J., Wijffels, S.E., Gordon, A.L., Ffield, A., Molcard, R., Susanto, R.D., Soesilo, I., Sopaheluwakan, J., Surachman, Y. and van Aken, H.M., 2004: INSTANT: A new international array to measure the Indonesian Throughflow, Eos Trans. AGU, 85(39), 369–376, doi:10.1029/2004EO390002.

Sprintall, J., Wijffels, S.E., Molcard, R. and Jaya I., 2009: Direct estimates of the Indonesian Throughflow entering the Indian Ocean: 2004–2006, J. Geophys. Res., 114, C07001, doi:10.1029/2008JC005257.

Sprintall, J. and Revelard, A., 2014: The Indonesian throughflow response to Indo-Pacific climate variability, J. Geophys. Res. Oceans,119, 1161–1175, doi:10.1002/2013JC009533.

Susanto, R.D., Ffield, A., Gordon, A.L. and Adi, T.R., 2012: Variability of Indonesian throughflow within Makassar Strait, 2004–2009, J. Geophys. Res., 117, C09013, doi:10.1029/2012JC008096.

Susanto, R.D., Wei, Z., Adi, T.R., Zheng, Q., Fang, G., Fan, B., Supangat, A., Agustiadi, T., Li, S., Trenggono, M. and Setiawan, A., 2016: Oceanography surrounding Krakatau Volcano in the Sunda Strait, Indonesia. Oceanography 29(2):264–272, http://dx.doi.org/10.5670/oceanog.2016.31.

Thoppil, P.G., Metzger, E.J., Hurlburt, H.E., Smedstad, O.M. and Ichikawa, H., 2016: The current system east of the Ryukyu Islands as revealed by a global ocean reanalysis. Progress in Oceanography 141, 239–258.

Tokinaga, H., Xie, S.-P., Timmermann, A., McGregor, S., Ogata, T., Kubota, H. and Okumura, Y.M., 2012: Regional patterns of tropical Indo-Pacific Climate change: Evidence of the Walker Circulation weakening, J. Clim., 25, doi:10.1175/JCLI-D-11-00263.1.

van Aken, H.M., Brodjonegoro, I.S. and Jaya, I., 2009: The deep-water motion through the Lifamatola Passage and its contribution to the Indonesian throughflow. Deep Sea Research Part I: Oceanographic Research Papers. 56. 1203-1216.

Vecchi, G.A., Soden, B.J., Wittenberg, A.T., Held, I.M., Leetma, A. and Harrison, M.J., 2006: Weakening of tropical Pacific atmospheric circulation due to anthropogenic forcing, Nature, 441, 73–76, doi:10.1038/nature04744.

Wainwright, L., Meyers, G., Wijffels, S. and Pigot, L., 2008: Change in the Indonesian Throughflow with the climatic shift of 1976/77, Geophys. Res. Lett., 35, L03604, doi:10.1029/2007GL031911

Wheeler, M.C. and Hendon, H.H., 2004: An All-Season Real-Time Multivariate MJO Index: Development of an Index for Monitoring and Prediction. Mon. Wea. Rev., 132, 1917–1932, https://doi.org/10.1175/1520-0493(2004)132<1917:AARMMI>2.0.CO;2

Wijffels, S. and Meyers, G., 2004: An intersection of oceanic wave guides: Variability in the Indonesian Throughflow region,J. Phys.Oceanogr.,34, 1232–1253.

Yoneyama, K., Zhang, C. and Long, C.N., 2013: Tracking Pulses of the Madden–Julian Oscillation. Bull. Amer. Meteor. Soc., 94, 1871–1891, https://doi.org/10.1175/BAMS-D-12-00157.1

Yu, Z., Metzger, E.J., Thoppil, P., Hurlburt, H.E., Zamudio, L., Smedstad, O.M., Na, H., Nakamura, H. and Park, J-H., 2015: Seasonal Cycle of Volume Transport through Kerama Gap Revealed by a 20-year Global HYbrid Coordinate Ocean Model Reanalysis. Ocean Modelling. 96. 10.1016/j.ocemod.2015.10.012.

Zhang, C., 2005: Madden-Julian Oscillation, Rev. Geophys., 43, RG2003, doi:10.1029/2004RG000158.

Zhang, C., Gottschalck, J., Maloney, ED., Moncrieff, M.W., Vitart, F., Waliser, D.E., Wang, B. and Wheeler, M.C., 2013: Cracking the MJO nut, Geophys. Res. Lett., 40, 1223–1230, doi:10.1002/grl.50244.

Zhang, Q., Gottschalck, J. and Xue, Y., 2019: EXTENSION OF THE CPC MJO INDEX TO FORECAST MODE.

Zhou, L. and Murtugudde, R., 2010: Influences of Madden–Julian Oscillations on the eastern Indian Ocean and the maritime continent. Dynamics of Atmospheres and Oceans. 50. 257-274. 10.1016/j.dynatmoce.2009.12.003.